Geoderma 454 (2025) 117194

Contents lists available at ScienceDirect

Geoderma

journal homepage: www.elsevier.com/locate/geoderma

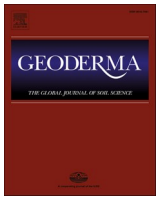

Gross soil N transformations and microbial communities in Luxembourg beech forest (*Fagus sylvatica L.*) soils along a pH gradient

Mengru Jia [a,*], Annemieke Kooijman [a], Roland Bol [a,b], Wim W. Wessel [a], Kathrin Hassler [a], Albert Tietema [a]

[a] Institute for Biodiversity and Ecosystem Dynamics, University of Amsterdam, Science Park 904 1098 XH Amsterdam, the Netherlands
[b] Institute of Bio- and Geosciences, IBG-3: Agrosphere, Forschungszentrum Jülich GmbH 52425 Jülich, Germany

ARTICLE INFO

Handling Editor: D. Said-Pullicino

Keywords:
Gross N transformations
15N tracing
Soil pH
Microbial N demand
Fungi-to-bacteria ratios
N fertility
Organic layer
Mineral topsoil

ABSTRACT

Acidic and calcareous soils differ in nitrogen (N) cycling, yet the underlying gross N transformations remain unclear in temperate forests. To address this gap, we quantified gross N transformations and microbial abundances in the organic layer and mineral topsoil (0–5 cm) of four closely situated beech forests along a natural pH gradient. Gross N turnover accelerated from acidic to calcareous soils, with gross mineralization rates increasing 6-fold in the organic layer and 10-fold in the mineral topsoil. However, net N release did not increase accordingly due to concurrent increases in gross immobilization. Enhanced immobilization at higher pH reflected greater microbial N demand under bacterial dominance, evidenced by higher microbial N, lower microbial C:N ratios and reduced fungi-to-bacteria (F:B) ratios. Autotrophic nitrification also increased with pH, corresponding to elevated ammonium supply from gross mineralization and higher abundances of ammonia-oxidizers. Heterotrophic nitrification was much lower than autotrophic nitrification in calcareous soils but equally important in acidic soils. Net N release was restricted to the mineral topsoil, shifting from low ammonium and nitrate release in acidic soils, to substantial nitrate release in calcareous soils, potentially supporting greater plant species richness at high pH. Our results demonstrate that soil N supply mechanisms differ markedly along the pH gradient, from low immobilization at low pH to high nitrification at high pH, driven by shifts in fungal versus bacterial dominance and their distinct N demands. This improved understanding of microbial regulation of acidity-related soil N fertility is crucial for predicting forest responses to global climate disturbances.

1. Introduction

Temperate forests cover approximately half of Europe's land area and provide essential ecosystem services, including wood supply, biodiversity conservation, and carbon (C) sequestration (Forest Europe, 2020; Djemiel et al., 2023). Soil nitrogen (N) availability, particularly in its mineral N forms, i.e., ammonium (NH_4^+) and nitrate (NO_3^-), often limits plant growth and productivity in these forests (Lang et al., 2021; Vitousek et al., 2022). However, when N inputs exceed ecosystem demands or storage capacity, losses through leaching or gaseous emissions may occur, leading to soil acidification, reduced biodiversity, and exacerbated climate change (de Vries et al., 2021; Templer et al., 2012). European temperate forests are particularly susceptible to N loss due to historical N deposition, and this issue is likely to worsen with increasing forest disturbances driven by intensive forest management (Clark et al., 2019), extreme weather events (Krüger et al., 2021), and global warming (Schmitz et al., 2019). To evaluate forest N status and predict ecosystem responses to future global changes, it is essential to understand the patterns and controls of soil N transformation processes (Zhang et al., 2018; Elrys et al., 2023).

Soil microbes play a crucial role in regulating N transformation processes, influenced by a combination of climate and soil properties (Booth et al., 2005; Elrys et al., 2023). In the wet temperate climate zone of Europe, soil properties, particularly pH, strongly influence microbial communities and the N transformations they mediate (Michalet and Liancourt, 2024). Fungi typically dominate acidic soils, while bacteria tend to prevail in neutral to alkaline conditions (Strickland and Rousk, 2010; Rütting et al., 2013). It is commonly believed that the slower, fungi-dominated decomposition pathways of soil organic matter in acidic soils result in lower net N release compared to bacterial-dominated calcareous soils (Högberg et al., 2014; Neina, 2019). However, empirical support for this theory is limited, and many studies

* Corresponding author.
E-mail address: m.jia@uva.nl (M. Jia).

https://doi.org/10.1016/j.geoderma.2025.117194
Received 18 July 2024; Received in revised form 23 January 2025; Accepted 27 January 2025
Available online 4 February 2025

suggest the opposite. For instance, some research indicates that fungi-dominated systems may not necessarily result in lower N leaching losses than bacteria-dominated ones (Rousk and Frey, 2015; de Vries et al., 2021). In temperate forests, net mineralization rates (the sum of inorganic N release) are often highest in acidic soils (Andrianarisoa et al., 2009; Leberecht et al., 2016; Kooijman et al., 2018b). In fact, slower N turnover does not always equate to lower net N release (Stark and Hart, 1997; Verchot et al., 2001), because net N transformations reflect only the balance of concurrent gross N transformation processes (Hart et al., 1994a; Staelens et al., 2012). The consumption of NH_4^+ and NO_3^-, particularly through microbial immobilization, can occur at rates comparable to or much lower than their production (i.e., gross mineralization and nitrification), leading to either low or high net N release (Corre et al., 2003; Rütting et al., 2015). In acidic soils, although gross N mineralization is low, the lower N demand of fungi, due to their generally higher C:N ratios than bacteria (Griffin, 1985), may still result in high net N mineralization (Robertson and Groffman, 2024). In contrast, in calcareous soils, high gross N mineralization rates may be counteracted by elevated bacterial N immobilization (Andrianarisoa et al., 2009; Kooijman et al., 2018b). However, gross N transformation processes remain largely unexamined in temperate forests with acidic versus calcareous soils. Moreover, while fungal or bacterial dominance is known to affect soil N retention (de Vries et al., 2012; de Vries and Bardgett, 2016), the fungi-to-bacteria (F:B) ratios have rarely been simultaneously measured alongside gross N transformation rates across broad pH gradients. A few studies have linked gross mineralization to F:B ratios in forest soils with varying pH, but they could not exclude the effects of climate (Elrys et al., 2021a) or N fertilizer application (Högberg et al., 2007). These knowledge gaps complicate our understanding of the microbial controls on internal N cycling in acidic versus calcareous forest soils.

Nitrification is typically associated with N loss, due to the high mobility of NO_3^- and its link to leaching and gaseous emissions (Elrys et al., 2021b; Rütting et al., 2021). However, in oxygen-rich temperate forests, nitrification also provides essential nutrients to understory vegetation (Andrianarisoa et al., 2010; Kooijman, 2010), particularly in calcareous soils where high plant species richness coincides with a preference for NO_3^- over NH_4^+ (Falkengren-Grerup, 1995; Diekmann and Falkengren-Grerup, 1998). Net nitrification rates often increase from acidic to calcareous soils, but the underlying gross nitrification pathways may differ across pH gradients (Gao et al., 2022; Zhang et al., 2023). In acidic soils, heterotrophic nitrification of organic N, primarily by fungi, often contributes significantly to NO_3^- production (Li et al., 2018; Martikainen, 2022). In contrast, calcareous soils with higher pH can enhance autotrophic nitrification by promoting the activity of ammonia-oxidizing archaea (AOA) and bacteria (AOB), which perform the rate-limiting step of this process (Rütting et al., 2021; Gao et al., 2022). Additionally, "comammox" bacteria, which oxidize ammonia to NO_3^- in a single cell, may also contribute to autotrophic nitrification, although their pH sensitivity is not yet well understood (Li et al., 2020; Osburn and Barrett, 2020). The relative contributions of autotrophic and heterotrophic pathways to gross nitrification and their responses to pH were compared in a manipulated pH gradient by Zhang et al. (2020). Similar comparisons in natural forests could provide further insights into the different nitrification pathways and their significance for ecosystem-specific N supply in acidic and calcareous soils.

Gross N transformations are typically quantified by ^{15}N pool dilution (Ribbons et al., 2016; Braun et al., 2018), in which total gross production and consumption fluxes are frequently calculated using analytical equations (Hart et al., 1994b; Hu et al., 2019). However, this method often cannot distinguish specific N transformation processes, such as microbial immobilization and different nitrification pathways (Schimel, 1996; Mary et al., 1998). The ^{15}N tracing approach with mirror labelling addresses this limitation by quantifying process-specific gross N transformation rates (Barraclough, 1997; Rütting et al., 2011, Rütting et al., 2021). *In situ* ^{15}N tracing allows for measuring gross N transformations under field conditions, including the presence of plant roots, over extended periods. In contrast, laboratory incubations provide controlled conditions with homogenized moisture and temperature, suitable for studying short-term internal N dynamics (Tietema and Wessel, 1992; Braun et al., 2018). Though soil sieving and the absence of plant roots may stimulate microbial activity (Murphy et al., 2003; Luxhøi et al., 2005), cross-ecosystem laboratory comparisons provide valuable insights into ecosystem-specific N cycling mechanisms (Fisk et al., 1998; Elrys et al., 2023). Despite this, the ^{15}N tracing technique remains less commonly used in current soil N transformation studies due to intensive sampling requirements and the need for extensive chemical analyses (Barraclough, 1991; Rütting et al., 2011).

In the Luxembourg cuesta landscape, characterized by a wet temperate climate, soils exhibit a clear gradient from acidic to more neutral (calcareous) conditions over a short distance (Kooijman, 2010; Cammeraat et al., 2018; Kausch and Maquil, 2018). Along this gradient, natural beech (*Fagus sylvatica* L.) forests have developed for over 100 years, offering a unique opportunity to investigate N dynamics between acidic and calcareous soils in mature forests under the same climate with litter from the same tree species. Here, we aim to investigate soil N supply patterns and underlying mechanisms in acidic versus calcareous soils. We selected four beech forests located on different parent materials to represent a natural pH gradient. We measured process-specific gross N transformation rates using laboratory ^{15}N tracing with mirror labelling, and combined these measurements with qPCR quantification of the abundance of bacteria, fungi, and autotrophic nitrifiers. We hypothesized that: (i) Both gross mineralization and microbial immobilization rates increase from acidic to calcareous soils, which is linked to a decrease in the fungi-to-bacteria (F:B) ratio and an increase in microbial N demand. Consequently, net mineralization decreases from acidic to calcareous soils due to increased immobilization. (ii) Heterotrophic nitrification dominates NO_3^- production in acidic soils, while autotrophic nitrification increases with the abundance of ammonia-oxidizers at higher pH. This leads to higher net nitrification and supports greater vegetation species richness in calcareous soils.

2. Materials and methods

2.1. Study sites, soil sampling, and chemical analysis

The four beech (*Fagus sylvatica* L.) forests were selected near Diekirch, Luxembourg, all located within approximately 25 km of each other and characterized by a similar, temperate, and humid climate (Cammeraat et al., 2018; Kooijman et al., 2018a). The mean temperature is 0.8 °C in January and 17.2 °C in July, with an annual rainfall of 788 mm. These forests have remained relatively undisturbed, with management limited to the occasional removal of large trees. The selected sites included two acidic forests on acidic sandstone (AS) and acidic loam (AL), and two calcareous forests on calcareous marl (CL) and limestone (LS). Site characteristics and locations are detailed in Table 1 and Fig. S1.

Samples for laboratory incubation experiments were collected in March 2022. In each beech forest, plots were randomly selected with four replicates per site in the forest interior. To approximate comparable litter quality, all study plots were located in mature beech monocultures, predominantly comprising trees with a diameter at breast height (DBH) greater than 50 cm. After removing all freshly fallen litter (from fall 2021), the organic layer (Org) was sampled in two 25 × 25 cm squares. The mineral topsoil (Ah) was then sampled within each 25 × 25 cm square, using six metal rings, each with a 5 cm diameter and a depth of 5 cm, encompassing the entire Ah horizon. On limestone, only the mineral topsoil was sampled, as the entire organic layer had been mixed into the mineral soil layer due to high earthworm activity. After sampling, the soil samples were homogenized by hand and sieved through a 4 mm mesh. Sieved samples intended for molecular analysis were frozen at −20 °C, and the remainder was stored at 4 °C for physical–chemical

Table 1
Forest and soil characteristics of selected Luxembourg beech forests in the current study.

Forest	AS	AL	CL	LS
Parent material	Acid sandstone	Acid loam	Calcareous marl	Dolomitic limestone
Soil Texture	loamy-sand	loam	clay-loam	clay-loam
Soil Type	Cambic Arenosol	Dystric Luvisol	Calcaric Cambisol	Regosol
Soil Profile	Ah-E-Bw-C	Ah-E-Bt-C	Ah-Bw-C	Ah-C
Humus Form	mormoder	mullmoder	vermimull	mull
Thickness of organic layer	4	4	2	–
Litter decay constant	0.16	0.34	1.21	n.d.
Forest Type	Fago-Quercetum	Fago-Quercetum	Carici-Fagetum	Carici-Fagetum
Location	Eppeldorf	Bigelbach	Ermsdorf	Moestroff
Coordinates	N 49°50′23″ E 06°15′53″	N 49°51′28″ E 06°17′48″	N 49°50′14″ E 06°13′45″	N 49°52′25″ E 06°14′32″

Data was derived from Kooijman et al. (2008, 2009) and Cammeraat et al. (2018).

analysis.

Soil pH was determined in water, using a 1:2.5 (w:v) ratio for organic layer samples and a 1:10 (w:v) ratio for mineral topsoil based on dry mass. Soil moisture was measured gravimetrically. Soil organic matter (SOM) was measured via loss on ignition at 350 °C (Roper et al., 2019). Soil total C and N contents were measured in finely ground, air-dried soils using a CNS analyzer (Vario EL analyzer, Elementar), and soil C: N ratio was then calculated.

2.2. Microbial biomass, respiration, and population

Soil microbial C and N were measured using a 24-hour fumigation-extraction. Microbial C and N concentrations were calculated as the difference in organic C and total N in the 0.05 M K_2SO_4 extracts between fumigated and non-fumigated samples, corrected by extraction factors of 0.45 and 0.54, respectively (Brookes et al., 1985; Vance et al., 1987). Soil respiration was measured in a 20-day laboratory incubation at 20 °C in the dark, using a Respicond respirometer (Nordgren, 1988).

For molecular analysis, DNA was extracted from 0.25 g of frozen, moist samples using the DNeasy PowerSoil Pro Kit (Qiagen, USA) following the manufacturer's instructions. DNA quality and concentrations were estimated using the Qubit dsDNA BR Assay Kit (Invitrogen, USA). Quantitative real-time PCR was conducted in triplicate on each soil DNA sample (CFX Connect Real-time PCR Detection System Bio-Rad, USA) to determine the copy numbers of 16S rDNA, the ITS (internal transcribed spacer) region of fungal rDNA, and AOA and AOB *amoA*. The bacterial 16s rRNA gene was amplified with primers 515F and 806R targeting the V4 region. This primer set amplifies nearly all bacterial taxa with few biases, and has been commonly used to assess bacterial communities across soil pH gradients and ecosystems (Liu et al., 2007; Bergmann et al., 2011; Caporaso et al., 2011; Zhalnina et al., 2015). The ITS1 region of the fungal genomes was amplified using primers ITS1 and qITS2, enabling amplification of the widest possible range of fungi (White et al., 1990; Wakelin et al., 2007; Baldrian et al., 2013). The AOA *amoA* gene was amplified with primers Arch-amoAF and Arch-amoAR (Francis et al., 2005), and the AOB amoA gene was amplified with primers amoA-1F and amoA-2R (Rotthauwe et al., 1997). The 20 μL reaction mixture contained 4 μL 5 × HOT FIREPOl EvaGreen® Mix Plus (ROX), 0.5 μL of each primer (10 μM), 8 μL of diluted DNA template (80 ng), and 7 μL of sterile H_2O. The thermal cycling conditions are provided in Table S1 (Ribbons et al., 2016; Diao et al., 2023). The specificity of the qPCR reactions was determined by melting curve analysis and 1 % agarose gel electrophoresis. The standard curve for determining the gene copy number was made with purified PCR products (Ribbons et al., 2016, 2018).

2.3. Gross N transformations

Soil microcosms were established in 250-ml bottles, each containing sieved fresh soils equivalent to 6 g dry weight, adjusted to optimal gravimetric moisture levels (300 % for organic and 50 % for mineral soil samples; Tietema, 1992). The bottles were pre-incubated for 1 week at 20 °C in the dark. Oxic conditions were maintained by loosely covering the bottle lids and regularly uncapping, and water loss was measured. After pre-incubation, two "paired" ^{15}N experiments were conducted using the mirror-labelling (Barraclough, 1997; Mary et al., 1998; Rütting et al., 2021). Soil microcosms received either $^{15}NH_4NO_3$ or $NH_4^{15}NO_3$, each containing a ^{15}N fraction of 10 atom%, at a rate of 50 mg N kg^{-1} dry soil in a 1-ml solution. This application resulted in an initial ^{15}N fraction of 1–10 atom % in the NH_4^+ or NO_3^- pool. This concentration was chosen based on a pre-experiment, ensuring NH_4^+ and NO_3^- concentrations were sufficiently high for accurate measurement of ^{15}N abundances in all soil samples. The amount of N added was comparable to previous studies (Cheng et al., 2013; Zhang et al., 2022). Tracers were evenly distributed over the soil surface, with minimal soil disturbance to reduce potential effects on rate estimates (Hart et al., 1994a). Soil was extracted immediately (<10 min) (T_0), or after 6 (T_1), 24 (T_2) and 48 (T_3) hours following ^{15}N application using a 0.05 M K_2SO_4 solution (1:10, w:v) and shaken for 1 h. After filtration, NH_4^+ and NO_3^- concentrations were measured as previously described. Soil moisture was checked gravimetrically before extraction.

For ^{15}N analysis in soil extracts, we used the diffusion method for NH_4^+ (Sørensen and Jensen, 1991; Lachouani et al., 2010) and the azide method for NO_3^- (Lachouani et al., 2010). The methods were chosen based on the guidelines provided by Jia et al (2022), considering criteria such as sample N concentrations and volume, available instruments and chemicals, and time limitations. In brief, NH_4^+ from soil extracts was diffused onto an acidified filter after adding magnesium oxide (MgO), and then analyzed using an Vario ISOTOPE cube EA (Elemental Analyzer) connected to a Vision IRMS (Elementar, Germany). For NO_3^-, the ^{15}N abundances were determined by converting it to N_2O using a vanadium(III)-azide buffer, followed by measurement via a Trace Gas unit coupled to an Isoprime100 IRMS (Elementar, Germany). Net rates of NH_4^+ and NO_3^- release were derived from linear regression of NH_4^+ and NO_3^- concentrations over the ^{15}N incubation period, respectively. Net mineralization rates were calculated as the daily changes in total mineral N (i.e. sum of NH_4^+ and NO_3^-).

2.4. Data analysis

2.4.1. ^{15}N numeric model

The computer program used to calculate gross N transformations was adapted from Wessel and Tietema (1992). It employs a numerical simulation model with a variable time-step numerical integration procedure to simulate the paired ^{15}N experiments, and a simplex algorithm to iteratively find the best values for the model parameters. Using initial concentrations and ^{15}N abundances of the mineral N pools as input, the simplex algorithm fits the gross N transformation rates during model simulation. The calculation is based on the "isotopic exchange" principle, which considers the isotopic dilution of the labeled N pool, isotopic enrichment of the unlabeled N pool and equilibration between the two pools (Wessel and Tietema, 1992; Mary et al., 1998; Rütting et al., 2011). The organic N pool was assumed to have a constant size and initial ^{15}N at natural abundance (0.366 atom%) (Wessel and Tietema, 1992). Optimization was based on the least sum of squares of the residuals (SSR) between modeled and measured values of both ^{15}N abundances and N concentrations of the mineral N pools at different time points (Wessel and Tietema, 1992). The program generated values and errors for the optimal parameter set with minimum SSR for samples from each sampling location of each forest.

To obtain the most appropriate model, we adjusted the number of N pools, processes and kinetic settings, considering our soil and incubation conditions. The optimal model was selected based on minimum SSR (Wessel and Tietema, 1992), Akaike's information criterion (AIC) (Cox et al., 2006), and the determination coefficient (R^2) (Table S2). The final model included five key N transformation processes, namely mineralization, NH_4^+ immobilization, autotrophic nitrification (nitrification$_{aut}$), NO_3^- immobilization and heterotrophic nitrification (nitrification$_{het}$) (Fig. 1). All processes were set as zero-order in the final model, which is also supported by previous findings on short-term incubation periods in forest soils (Myrold and Tiedje, 1986). The model also simulated the reversible chemical adsorption of NH_4^+, assuming that adsorbed NH_4^+ is not measurable but participates in NH_4^+ transformations similarly to unabsorbed NH_4^+. The fraction of adsorbed NH_4^+, derived from the differences between added and recovered $^{15}NH_4^+$ amount of the T_0 samples (Table 2), was used as a parameter in the model. Remineralization of labeled N was considered negligible within the short-term experimental setting (Braun et al., 2018). Dissimilatory nitrate reduction to ammonium (DNRA) was excluded, as no visible ^{15}N inflow into the NH_4^+ pool was observed. Autotrophic nitrification was treated as a one-step process, as NO_2^- concentrations were found to be negligible (Staelens et al., 2012).

Gross N transformation rates fitted by the model were on a dry weight basis (mg N kg^{-1} dry soil day^{-1}), and were then converted to a C basis (mg N kg^{-1}C day^{-1}) and an areal basis (g N m^{-2} day^{-1}) based on the measured total C concentrations and bulk density. Averaged gross N transformation rates were calculated based on fittings from four field replicates, with standard errors provided.

2.5. Mean residence time (MRT)

The MRT indicates the average duration a N atom remains within a specific pool. A lower MRT signifies a faster turnover rate and thus a more dynamic pool. MRTs of soil NH_4^+, NO_3^-, and microbial N pools were calculated as the ratio of the pool size to its total inflows (i.e. production rates) (Booth et al., 2005; Corre et al., 2007). The calculations are as follows: MRT of NH_4^+ = NH_4^+ pool/gross mineralization; MRT of NO_3^- = NO_3^- pool/gross nitrification = NO_3^- pool/(nitrification$_{aut}$ + nitrification$_{het}$); MRT of microbial N = microbial N pool/total N immobilization. For calculations of MRTs, all relevant N transformation processes were expressed in units of mg N kg^{-1}C day^{-1}, and all relevant pools were expressed in units of mg N kg^{-1}C. All MRTs were expressed in units of days.

2.6. Statistical analysis

All statistical analyses of the data were performed using R version 4.3.2, and all data were checked for normality and log-transformed where necessary. One-way analysis of variance was used to compare site and microbial characteristics within each layer. Pair wise comparisons of means were performed using Tukey's Honestly Significant Difference (HSD) test at a significance level of $\alpha = 0.05$. The *t*-test was used to examine differences between the organic layer and mineral topsoil on the same parent material. For gross N transformation rates, non-overlapping 85 % confidence intervals (85 % CI) were used as an alternative criterion for detecting significant differences at $\alpha = 0.05$ (Payton et al., 2000; Rütting et al., 2010). All gross N transformation rates are presented as mean ± standard error of four field replicates.

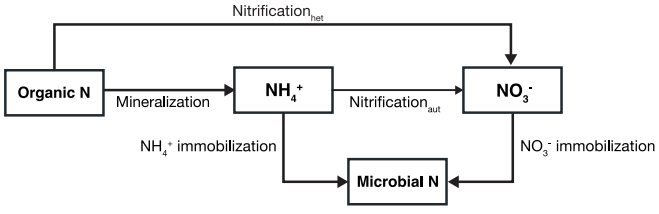

Fig. 1. Conceptual N cycle implemented in the numerical model. The model comprises four N pools and five transformations.

Table 2
Recovery of $^{15}NH_4^+$ and $^{15}NO_3^-$ immediately after their addition, respectively, for the organic layer and mineral topsoil samples of four Luxembourg beech forests on different parent materials.

Layer	Acidic sandy	Acidic loamy	Calcaric loamy	Limestone
Recovery of $^{15}NH_4^+$ after its addition				
Organic layer	128^b (4.69)	105^b (3.48)	71.3^a (3.70)	No organic layer
Mineral topsoil	96.5^c (0.63)	96.7^c (0.13)	79.4^a (2.23)	88.3^b (2.54)
Recovery of $^{15}NO_3^-$ after its addition				
Organic layer	122^a (3.94)	113^a (4.31)	121^a (0.54)	No organic layer
Mineral topsoil	84.2^a (1.01)	83.7^a (0.77)	86.0^a (0.65)	88.2^a (1.29)

Values in the brackets indicate standard error (n = 4); For each parameter, values followed by the same lowercase letter are not significantly different among soil types within each layer ($p < 0.05$).

To explore relationships between site characteristics, microbial abundances and gross N transformation rates, we conducted a principal component analysis (PCA) with soil physicochemical parameters as data points and microbial parameters as supplementary variables. The ordination scores from the first two PCA axes, labeled "soil PC1" and "soil PC2", were used to represent variations in soil properties and subsequently regressed against gross N transformation rates. Relationships between gross rates and specific microbial characteristics (e.g., microbial C:N ratios, fungal-to-bacteria abundance ratios, and *amoA* gene abundances) were further examined using linear regression. Finally, we used partial least squares path modelling (PLS-PM) to examine the hypothesized relationships among soil pH, microbial parameters, and gross and net N transformation rates, using the *pls-pm* package (Sanchez et al., 2017; Li et al., 2021). PLS-PM is a non-parametric method that uses partial least squares to explore relationships among variables, making it suitable for small sample sizes. Model composition was assessed using Goodness of Fit (GoF) statistics. Path coefficients, which indicate the direction and strength of linear relationships between latent variables, along with explained variability (R^2), were calculated using the "innerplot" function. Path coefficient significance was verified via bootstrapping (999 iterations), and standard errors and confidence intervals for constructs are provided in the Supplementary Information.

3. Results

3.1. Soil physicochemical properties

The four studied sites exhibited a wide pH range, from 4.39 to 6.81 in the organic layer and from 3.84 to 7.54 in the mineral topsoil, respectively (Table 3). The organic layer, when present, showed similar soil organic matter (SOM) content, total C and N concentrations, and C:N ratios (20.3–21.1) among sites. In the mineral topsoil, SOM increased from acidic to calcareous soils (1.56–2.47 kg m^{-2}). Total C and N differed significantly only between AL and CL when expressed as percentages, yet they increased from acidic to calcareous soils on an areal basis (Fig. S2). Soil C:N ratios in the mineral topsoil decreased with increasing pH (from 18.9 to 13.8). Soil NH_4^+ concentrations, measured on both a C and an areal basis, strongly decreased from acidic to calcareous soils in both the organic layer and the mineral topsoil. Conversely, soil NO_3^- concentrations increased with pH, but only in the mineral topsoil.

Table 3
Site characteristics of soil pH, soil organic matter (SOM), C and N concentrations, C:N ratios, extractable NH_4^+ and NO_3^- concentrations, microbial biomass, and respiration for the organic layer and mineral topsoil samples of four Luxembourg beech forests on different parent materials.

			AS	AL	CL	LS
Organic Layer	pH – H_2O	–	4.39^{a}	5.08^{b}	6.81^{c}	No organic layer
			(0.11)	(0.14)	(0.03)	
	SOM	kg m^{-2}	2.47^{a}	1.56^{a}	2.41^{a}	
			(0.17)	(0.26)	(0.78)	
	Total C	%	30.3^{ab}	25.7^{a}	35.8^{b}	
			(2.51)	(1.23)	(3.30)	
	Total N	%	1.49^{a}	1.27^{a}	1.70^{a}	
			(0.11)	(0.04)	(0.16)	
	C:N	g g^{-1}	20.3^{a}	20.3^{a}	21.1^{a}	
			(0.4)	(0.3)	(0.2)	
	Extractable NH_4^+	mg N kg^{-1}C	2509^{b}	2617^{b}	54^{a}	
			(783)	(625)	(3)	
	Extractable NO_3^-	mg N kg^{-1}C	1795^{a}	3894^{b}	1884^{a}	
			(190)	(530)	(176)	
	Microbial C	g C kg^{-1}C	5.23^{a}	5.13^{a}	4.48^{a}	
			(0.31)	(0.23)	(0.37)	
	Microbial N	g N kg^{-1}C	0.52^{a}	0.53^{a}	0.81^{a}	
			(0.09)	(0.13)	(0.09)	
	Microbial C:N	g g^{-1}	10.8^{a}	12.5^{a}	5.6^{a}	
			(1.43)	(3.61)	(0.30)	
	Respiration	g C kg^{-1}C day^{-1}	0.94^{a}	2.01^{b}	1.23^{a}	
			(0.12)	(0.15)	(0.07)	
Mineral topsoil	pH – H_2O	–	3.84^{c}	4.09^{c}	7.54^{a}	6.94^{b}
			(0.09)	(0.06)	(0.02)	(0.15)
	SOM	kg m^{-2}	3.18^{ab}	2.64^{a}	3.81^{b}	5.25^{c}
			(0.21)	(0.03)	(0.18)	(0.28)
	Total C	%	6.86^{ab}	4.49^{a}	8.40^{b}	5.95^{ab}
			(0.98)	(0.22)	(0.89)	(0.37)
	Total N	%	0.36^{ab}	0.24^{a}	0.51^{c}	0.43^{bc}
			(0.05)	(0.01)	(0.02)	(0.03)
	C:N	g g^{-1}	18.9^{b}	18.5^{b}	16.5^{b}	13.8^{a}
			(0.22)	(0.32)	(1.17)	(0.27)
	Extractable NH_4^+	mg N kg^{-1}C	1350^{b}	2277^{c}	6^{a}	4^{a}
			(288)	(263)	(3)	(3)
	Extractable NO_3^-	mg N kg^{-1}C	370^{a}	427^{a}	979^{a}	2113^{b}
			(135)	(241)	(86)	(40)
	Microbial C	g C kg^{-1}C	3.60^{a}	4.40^{ab}	6.20^{bc}	7.12^{c}
			(0.57)	(0.15)	(0.68)	(0.44)
	Microbial N	g N kg^{-1}C	0.20^{a}	0.45^{ab}	0.89^{bc}	1.14^{c}
			(0.02)	(0.15)	(0.13)	(0.14)
	Microbial C:N	g g^{-1}	18.5^{b}	12.5^{ab}	7.12^{a}	6.38^{a}
			(3.12)	(2.63)	(0.32)	(0.43)
	Respiration	g C kg^{-1}C day^{-1}	0.25^{a}	0.54^{b}	0.42^{ab}	0.64^{b}
			(0.07)	(0.07)	(0.05)	(0.06)

Values in the brackets indicate standard error (n = 4); For each parameter, values followed by different lowercase letters are significantly different among soil types within each layer; underlined values are significantly different between layers for each soil type ($p < 0.05$).

3.2. Microbial biomass, activity and population

Soil microbial characteristics varied strongly across the pH gradient. On both a C and an areal basis, soil microbial N approximately doubled from acidic to calcareous soils in the mineral topsoil (Table 3; Fig. S2). Microbial C:N ratios decreased from values above 10 in acidic soils to values around 5–7 in calcareous soils in both the organic layer and the mineral topsoil. When expressed on a C basis, laboratory-measured respiration rates were higher in the organic layer (0.94–1.23 g C kg^{-1}C day^{-1}) than in the mineral topsoil (0.25–0.64 g C kg^{-1}C day^{-1}). In the organic layer, respiration rates showed no clear trend with soil pH, whereas in the mineral topsoil, they increased from acidic to calcareous soils, particularly when expressed on an areal basis.

Bacterial abundances increased from acidic to calcareous soils in both the organic layer (on a C basis) and the mineral topsoil (on an areal basis) (Fig. 2; Fig. S3), correlating positively with respiration rates in both layers ($R^2 = 0.57$ and 0.62, $p < 0.05$). In contrast, fungal abundances decreased from acidic to calcareous soils on both measurement bases. Fungi-to-bacteria (F:B) abundance ratios decreased from acidic to calcareous soils, with values ranging from 1.48 to 0.08 in the organic layer and from 0.4 to 0.02 in the mineral topsoil. AOA and AOB abundances responded differently to pH: AOA abundances increased with pH in both layers, while AOB abundances increased only in the mineral topsoil, on both a C and an areal basis. Ratios of AOA to AOB gene abundances did not differ significantly ($p > 0.05$) among soil types probably due to high field variability, but they were positively correlated with pH in the organic layer (Fig. S3).

4. Gross N transformation rates and N turnover

4.1. Gross N transformation rates on a C basis

A good agreement was found between modelled and observed data (Fig. S4), indicating that the model used in this experiment ensured adequate representation of the system. On a C basis (mg N kg^{-1}C day^{-1}), gross N transformation rates clearly increased from acidic to calcareous soils (Fig. 3). Gross mineralization rates rose with pH from 82 to 492 mg N kg^{-1}C day^{-1} in the organic layer, and from 10 to 429 mg N kg^{-1}C day^{-1} in the mineral topsoil. Similarly, NH_4^+ immobilization rates increased across the pH gradient. In the organic layer, NH_4^+ immobilization rates ranged from 192 to 388 mg N kg^{-1}C day^{-1}, but did not differ significantly ($p > 0.05$) among sites probably due to field variability. In the mineral topsoil, NH_4^+ immobilization rates were negligible in acidic soils but surged to 77 and 573 mg N kg^{-1}C day^{-1} in the calcareous CL and LS soils, respectively.

Autotrophic nitrification rates increased from acidic to calcareous soils as well, rising from 18 to 165 kg^{-1}C day^{-1} in the organic layer and from 2 to 334 mg N kg^{-1}C day^{-1} in the mineral topsoil. Heterotrophic nitrification also contributed to gross nitrification, especially in the acidic soils. In the organic layer, this was observed only in the acidic AL soil (31 mg N kg^{-1}C day^{-1}), accounting for 43 % of gross nitrification. In the mineral topsoil, the contribution of heterotrophic nitrification decreased from 80–90 % in acidic soils to 18–40 % in calcareous soils, although the rates increased at higher pH. NO_3^- immobilization also increased along the pH gradient, from 140 to 234 mg N kg^{-1}C day^{-1} in the organic layer, and surged in the mineral topsoil from negligible levels in acidic soils to 106–198 mg N kg^{-1}C day^{-1} in calcareous soils. This process accounted for 25–33 % of gross immobilization in the organic layer, and 28–54 % in the mineral topsoil.

4.2. Gross and net N transformation rates on an areal basis

On an areal basis (g N m^{-2} day^{-1}), gross N transformation rates exhibited a similar increase from acidic to calcareous soils in both layers (Fig. S5). Gross mineralization rates increased with pH, ranging from 0.12 to 1.38 g N m^{-2} day^{-1} in total. It was the primary pathway for inorganic N production from organic N, occurring at rates 4–10 times higher than heterotrophic nitrification. The organic layer, when present, contributed 73–89 % of total gross mineralization, though its contribution decreased along the pH gradient. Gross N immobilization occurred at low pH only in the organic layer (0.32–0.37 g N m^{-2} day^{-1}). At high pH, the mineral topsoil accounted for 40 % of immobilization in

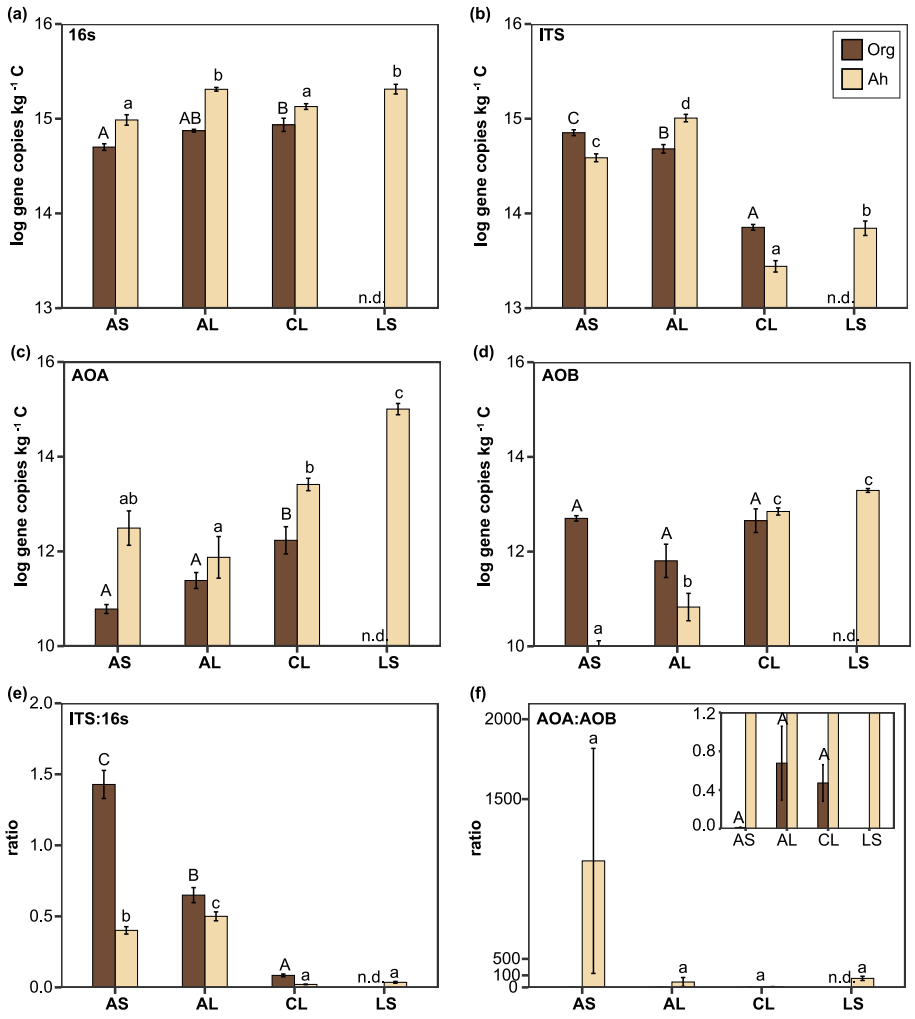

Fig. 2. Gene abundances expressed as log gene copies $kg^{-1}C$ for (a) bacterial 16 s, (b) fungal ITS, (c) AOA and (d) AOB, and ratio of (e) ITS:16 s (fungi-to-bacteria abundance ratio) and (f) AOA:AOB to pH in the organic layer (Org) and mineral topsoil (Ah) samples of four Luxembourg beech forests (mean and standard error, n = 4). Values followed by different uppercase or lowercase letters are significantly different among soil types within the organic layer or the mineral topsoil, respectively ($p < 0.05$).n.d.: no data.

the CL soil (1.1 g N m^{-2} day^{-1} in total) and fully contributed to immobilization in the LS soil (2.6 g N m^{-2} day^{-1} in total). NH_4^+ immobilization consistently exceeded NO_3^- immobilization, with rates increasing from 0.24 to 1.62 g N m^{-2} day^{-1} for NH_4^+ and from 0.08 to 0.59 g N m^{-2} day^{-1} for NO_3^- across the pH gradient. Autotrophic nitrification increased from 0.02 to 1.02 g N m^{-2} day^{-1} with higher pH, primarily occurring in the organic layer (78–88 %) at low pH and shifting to the mineral topsoil (56–100 %) at high pH. Heterotrophic nitrification also increased with pH (0.03–0.12 g N m^{-2} day^{-1} in total), with the mineral topsoil contributing half of this value in acidic AL soils and fully in all other soils.

In the organic layer, net mineralization was negative, and net nitrification did not differ significantly from zero during the laboratory incubation (Fig. 4). In the mineral topsoil, net mineralization averaged 0.05 g N m^{-2} day^{-1} in acidic soils, with equal contribution from NH_4^+ and NO_3^-. As pH rose, net mineralization decreased in this layer due to increased NH_4^+ immobilization. However, net nitrification increased to 0.06 and 0.17 g N m^{-2} day^{-1} in calcareous CL and LS soils, respectively.

4.3. Mean residence times

Gross N turnover accelerated from acidic to calcareous soils, as indicated by the decreasing mean residence times (MRTs) of various N pools (Table 4). In the organic layer, the MRT of NH_4^+ accelerated from 17–18 days in acidic soils to less than 1 day in calcareous soils. In the mineral topsoil, NH_4^+ MRT decreased from over 1 year to 3–18 days. Similarly, the MRT of NO_3^- in both layers decreased from 2–3 months in acidic soils to 10–14 days in calcareous soils. The MRT of microbial N decreased in the mineral topsoil from approximately 1 month to 1–5 days but did not vary in the organic layer. Overall, the organic layer showed much faster turnover of soil NH_4^+, NO_3^- and microbial N pools than the mineral topsoil.

5. Relationships between pH, microbial characteristics and N transformation rates

To identify potential drivers of gross N transformations, we performed a PCA on site characteristics and regressed the gross rates against the PCA axes (Fig. 5, fig S6). The first two PCA dimensions accounted for 95 % of the variation in soil physicochemical properties (Fig. 5 a-b). The first axis (soil PC1), explaining 65 % of the variation, was primarily driven by increases in soil C, N, and C:N ratios, which distinguished the mineral topsoil from the organic layer, and was negatively correlated with AOA abundances. The second axis (soil PC2), explaining 30 % of the variation, was mainly driven by high soil pH, which was correlated with increased microbial N, AOA, and AOB abundances, as well as decreased microbial C:N and F:B ratios.

Pairwise linear regression showed that gross mineralization,

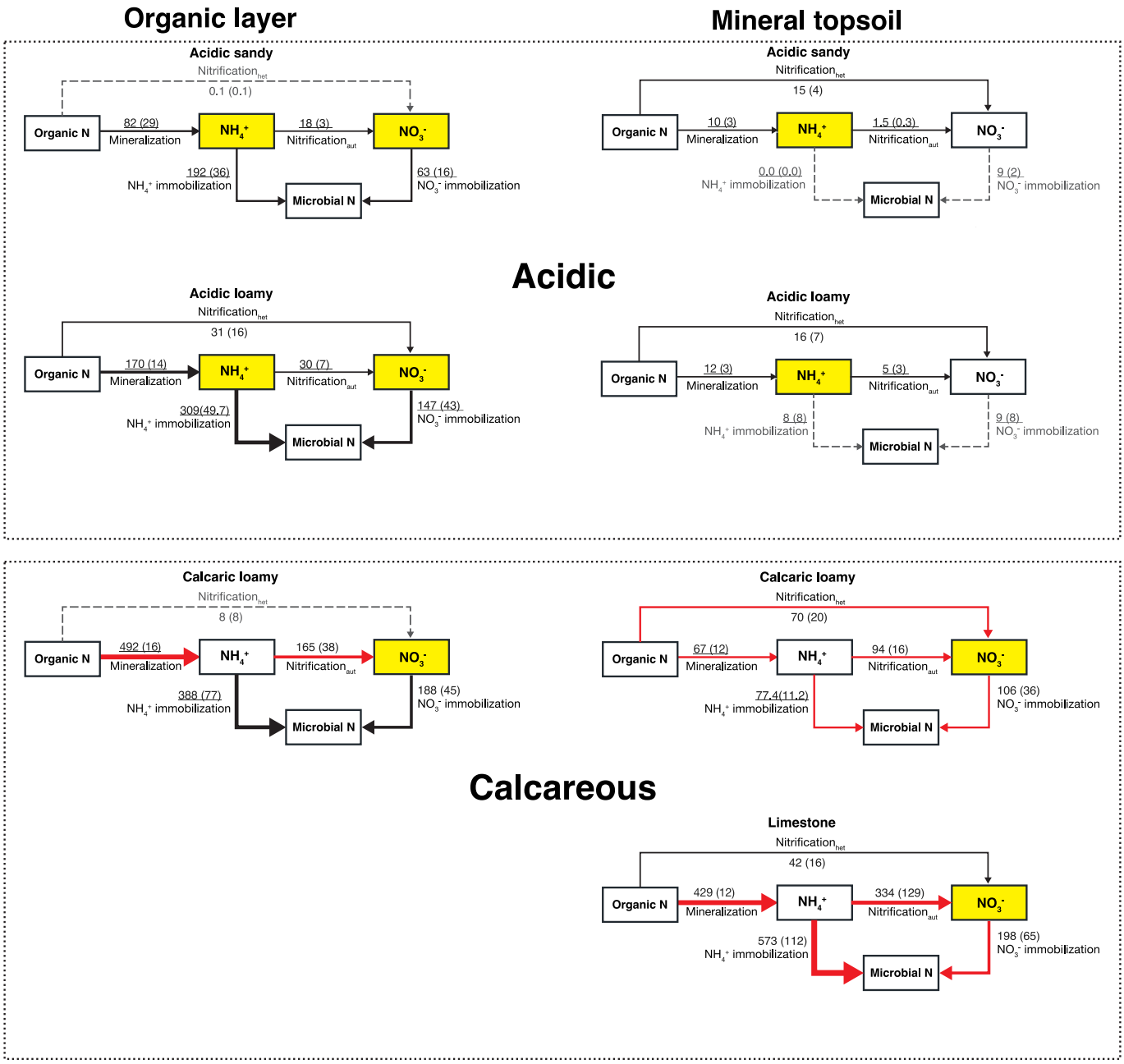

Fig. 3. Gross N transformations on a C basis (mg N $kg^{-1}C$ day^{-1}) in the organic layer and mineral topsoil of four Luxembourg beech forests with different soil types (mean with standard error in brackets; n = 4). Pools of dominated N species are highlighted. Underlined transformation rates were significantly different between the organic layer and mineral topsoil. Transformation rates shown as red lines in calcareous soils were significantly higher than those in acidic soils. Grey dashed lines indicate transformation rates not significantly different from 0. Thicker lines represent higher values.

immobilization and autotrophic nitrification on a C basis were all positively correlated with soil PC2 (Fig. 5 c-e), but they showed no relation to PC1, likely due to the normalization that accounted for variations in C content (Fig. 5 c-e; Fig. S6). Contributions of heterotrophic nitrification to total gross nitrification were negatively correlated with both PC1 and PC2, suggesting a greater importance of heterotrophic nitrification in acidic mineral topsoil (Fig. 5f; Fig. S6).

The relationships between gross N transformation rates and parameters of microbial abundances were evident within each layer. Specifically, gross mineralization, gross immobilization, as well as NH_4^+ and NO_3^- immobilization rates individually, were all negatively correlated with F:B ratios (Fig. S7). In the mineral topsoil, gross mineralization and immobilization were also negatively correlated with microbial C:N ratios. Autotrophic nitrification rates were positively correlated with AOA abundances in both layers and with AOB abundances in the mineral topsoil. Additionally, in the mineral topsoil, the contribution of heterotrophic nitrification to total gross nitrification was negatively correlated with microbial C:N and F:B ratios.

The partial least squares path model provided an integrated view of how microbial characteristics and N transformations varied along the pH gradient (Fig. 6). Specifically, soil pH positively affected gross N release (combining gross mineralization and heterotrophic nitrification) and negatively affected the F:B ratio, which, in turn, was negatively associated with gross immobilization. Net mineralization was positively influenced by gross N release but negatively affected by gross immobilization (Fig. 6 a). Furthermore, gross nitrification was positively influenced by *amoA* gene abundances, while NO_3^- immobilization was negatively affected by the F:B ratio. Net nitrification was positively

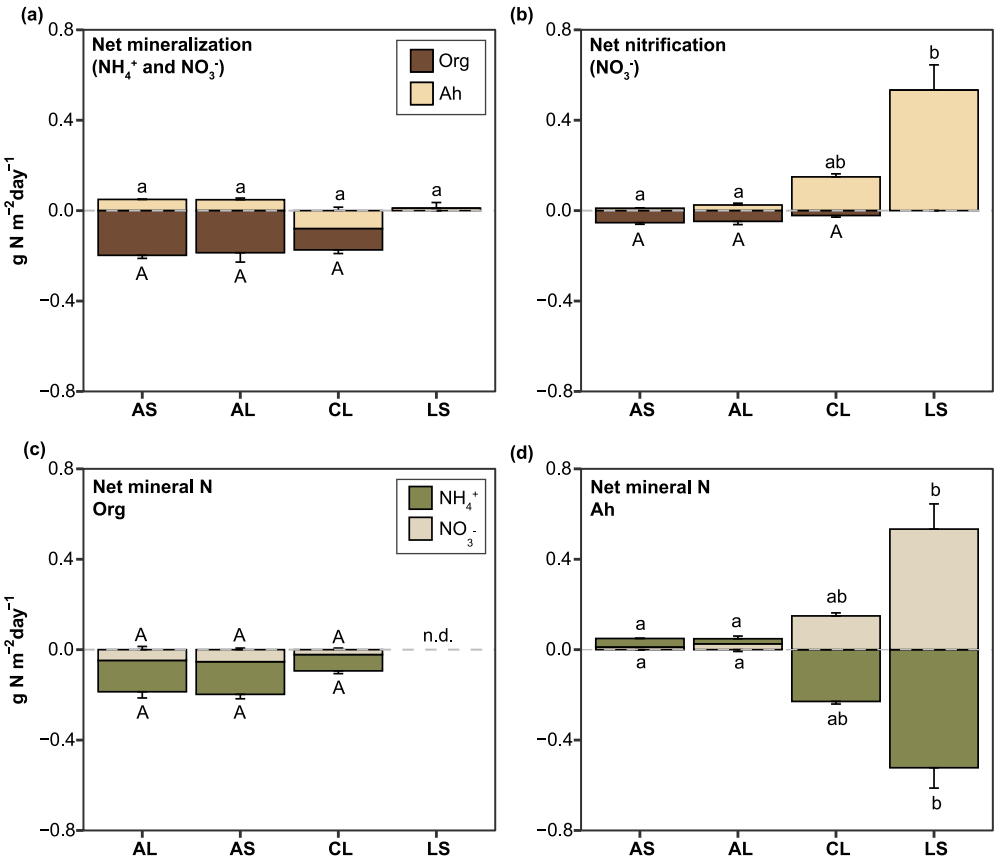

Fig. 4. Net rates on a m^2 basis of (a) mineralization and (b) nitrification in the organic layer (Org) and mineral topsoil (Ah) combined, and net release of NH_4^+ and NO_3^- in the (c) organic layer and (d) mineral topsoil separately (mean and standard error, n = 4). For a single process, values followed by different uppercase or lowercase letters are significantly different among soil types within the organic layer or the mineral topsoil, respectively ($p < 0.05$).

Table 4
Mean residence times (MRTs, day) of NH_4^+, NO_3^-, and microbial N during ^{15}N pool dilution incubation experiments for the organic layer and mineral topsoil of four Luxembourg beech forests.

		AS	AL	CL	LS
Organic layer	MRT of NH_4^+	18.2^b (4.9)	16.7^b (3.2)	1.0^a (0.3)	No organic layer
	MRT of NO_3^-	112^c (12)	60^b (4)	10^a (1.1)	
	MRT of microbial N	2.2^a (0.7)	1.2^a (0.2)	1.5^a (0.2)	
Mineral topsoil	MRT of NH_4^+	397^c (107)	559^c (234)	18^b (3.1)	3^a (0.2)
	MRT of NO_3^-	123^b (22)	141^b (59)	14^a (1.9)	14^a (4.8)
	MRT of microbial N	30.6^c (12.1)	39.8^c (30.6)	5.3^b (0.6)	1.6^a (0.4)

Values in the brackets indicate standard error (n = 4); For each parameter, values followed by different lowercase letters are significantly different among soil types within each layer; underlined values are significantly different between layers for each soil type ($p < 0.05$).

linked to gross nitrification and inversely related to NO_3^- immobilization (Fig. 6 b).

6. Discussion

6.1. Gross N transformations related to soil pH and F:B abundance ratios

Consistent with our first hypothesis, gross mineralization and immobilization increased from acidic to calcareous soils, correlating with declined microbial C:N and F:B ratios and increased microbial N. Gross mineralization was the main driver of gross N release from organic N (in comparison to heterotrophic nitrification), which aligns with previous studies in temperate deciduous forests (Tietema and Wessel, 1992; Staelens et al., 2012). The increased gross mineralization and immobilization at elevated pH may be driven by bacterial dominance, where high N demand promotes 'N mining' from organic N (Craine et al., 2007; Hicks et al., 2021) and enhances N immobilization in microbial biomass (Robertson and Groffman, 2024). Bacteria are expected to have higher N demands due to their lower microbial C:N ratios (Högberg et al., 2006), stricter stoichiometric constraints (Strickland and Rousk, 2010), and shorter life cycles (Rousk and Bååth, 2011) compared to fungi. We observed the lowest MRTs for both mineral N and microbial N pools in calcareous soils, also indicating high N demand and intense N competition compared to that in the acidic soils (Scott et al., 1998; Tahovská et al., 2013). The strong positive correlation between bacterial abundances and respiration further supported high microbial activity and potentially high N demand in bacterial-dominated soils (Kooijman et al., 2016, Kooijman et al., 2018b).

The relationships among soil pH, F:B ratios and gross mineralization rates observed in our study are consistent with those reported in a boreal forest study (Högberg et al., 2007). However, their research focused on the organic layer across a relatively narrow pH gradient of 4.9–5.3, using samples from different years and including plots fertilized with N. Also, they did not report responses of microbial immobilization and the consequences for soil N availability. In contrast, we investigated both the organic layer and mineral topsoil across a broader natural pH gradient (3.8–6.9) in beech forests. We found not only an increase in gross mineralization, but also an even stronger increase in microbial immobilization with rising pH — both driven by a shift from fungal to

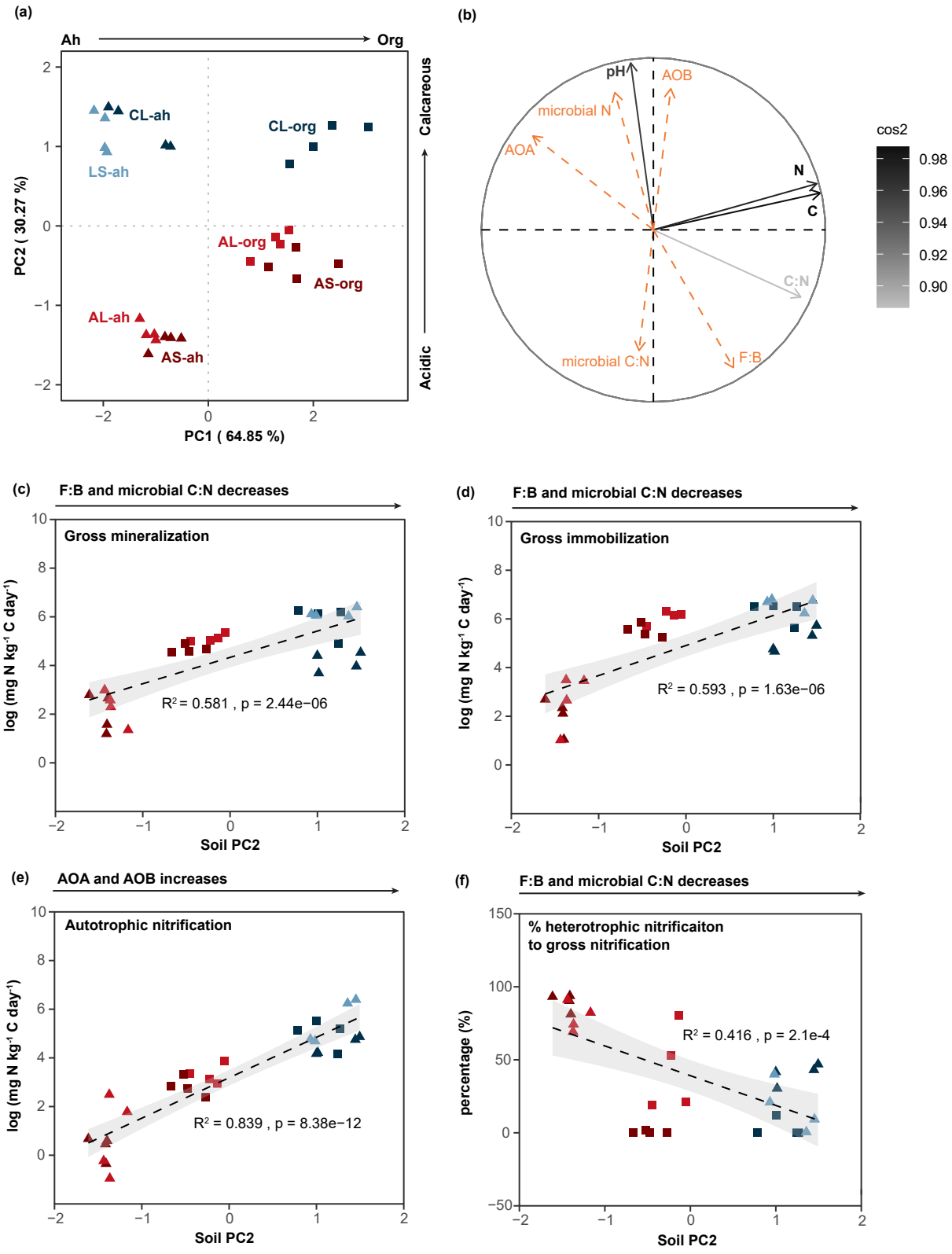

Fig. 5. Principal Component Analysis (PCA) of soil physio-chemical properties (pH, soil C, N, and C:N ratios from four Luxembourg beech forests with distinct soil types; microbial variables, including the microbial N (g N kg^{-1}C), microbial C:N ratio, F:B gene ratio, and gene abundances of AOA and AOB (log gene copies kg^{-1}C), were plotted as supplementary variables. (a) PCA showing coordinates of soils from the organic layer and mineral topsoil across the four forests on the first two axes. (b) Correlation biplot illustrating relationships between physio-chemical and microbial variables. Scores for the first two PCA axes were extracted, and regression of PCA axis 2 was performed against (c) gross mineralization, (d) gross immobilization, (e) autotrophic nitrification, and (f) the proportion of heterotrophic nitrification to total gross nitrification.

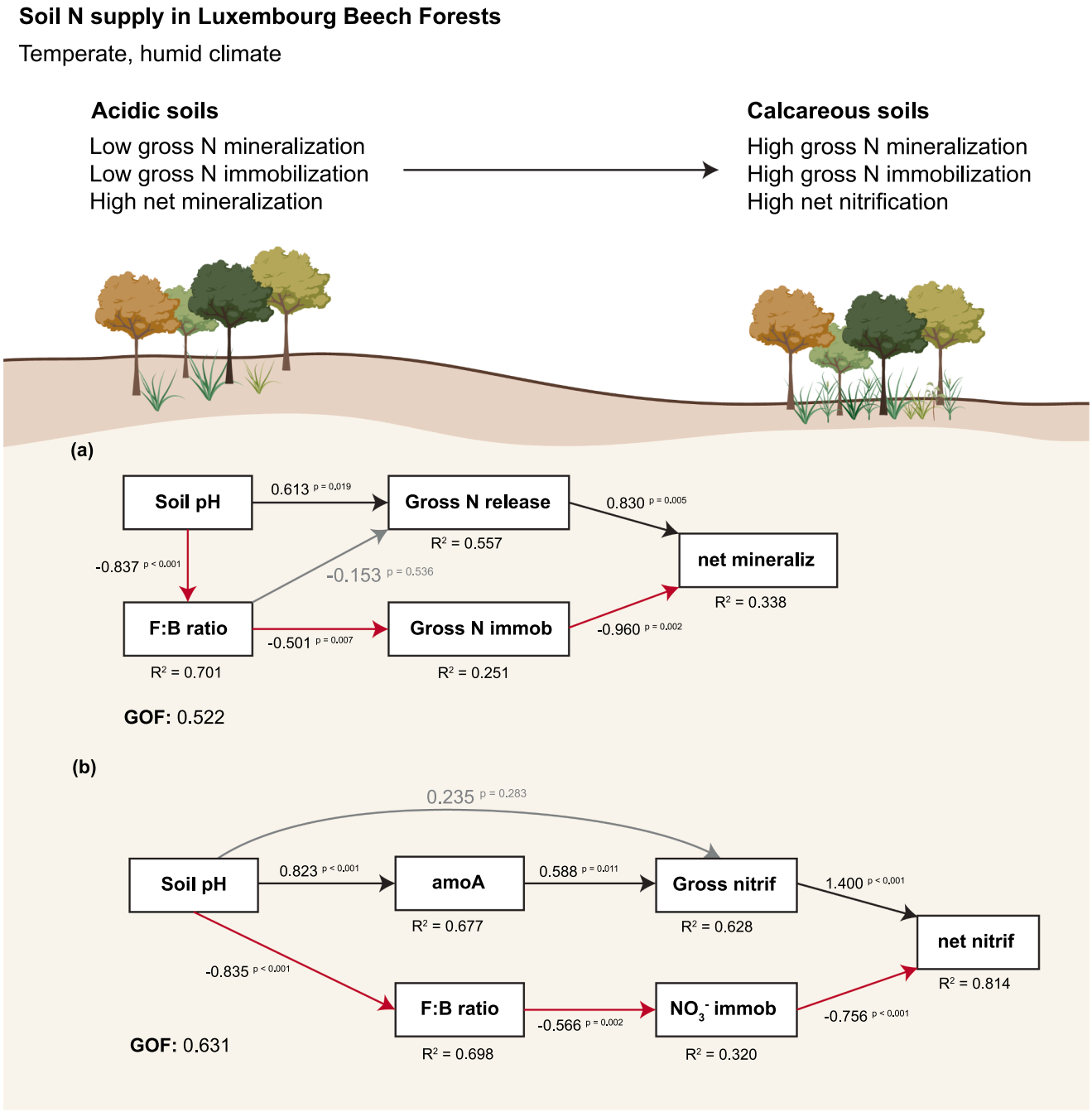

Fig. 6. Partial least squares path model (PLS-PM) showing the relationships between soil pH, microbial parameters, and rates of gross and net N transformations. (a) Relationships between soil pH, F:B ratio, gross N release, gross N immobilization, and net mineralization. (b) Relationships between soil pH, amoA gene abundances, F:B ratio, gross nitrification, NO_3 immobilization, and net nitrification. Gross N release is a latent variable comprising gross mineralization and heterotrophic nitrification; F:B ratio is a latent variable comprising F:B gene ratios and microbial C:N ratios; amoA is a latent variable comprising AOA and AOB gene abundances. Black and red lines indicate positive and negative relationships, respectively, while grey lines represent insignificant relationships ($p > 0.05$). Numbers next to each line are the correlation coefficients. R^2 values are placed below each variable to indicate the explained variance of each factor.

bacterial dominance. Consequently, net mineralization decreased from acidic to calcareous soils. To our knowledge, this is the first study to link gross immobilization with F:B ratios across the soil pH gradient, thereby providing a mechanistic explanation for the reduced net mineralization in calcareous soils observed in previous studies (Kooijman et al., 2008; Andrianarisoa et al., 2009). Our findings contradict the traditional view that fungal dominance results in higher N immobilization (de Graaff et al., 2010; de Vries et al., 2011), but aligns with recent research showing increased N immobilization in systems with low microbial C:N ratios (de Vries et al., 2021) or high bacterial growth (Rousk and Frey, 2015).

While NH_4^+ immobilization dominated the gross immobilization process (~70 %), both NH_4^+ and NO_3^- immobilization increased from acidic to calcareous soils. Notably, NO_3^- immobilization occurred only when NH_4^+ was net immobilized (negative NH_4^+ release), a pattern observed in both the organic layer and the calcareous mineral topsoil. These results suggest that microbes preferentially utilize NH_4^+ across all sites and immobilize NO_3^- mainly when NH_4^+ availability is insufficient to meet their N demands.

Overall, the gross mineralization and immobilization rates observed

in our study align with those previously reported in temperate forests across a wide pH gradient. At acidic sites, gross mineralization and NH_4^+ immobilization rates matched those in the organic layer (Tietema and Wessel, 1992; Corre et al., 2003; Ribbons et al., 2016) and mineral topsoil (Vervaet et al., 2004; Staelens et al., 2012) of similar temperate forests. This was also the case for the calcareous sites (Dannenmann et al., 2016; Ribbons et al., 2018). NO_3^- immobilization rates were within earlier ranges reported for temperate deciduous (Berntson and Aber, 2000; Bengtsson et al., 2003) and coniferous forests (Davidson et al., 1992; Stark and Hart, 1997).

6.2. Gross nitrification and NO_3^- availability

Consistent with our second hypothesis, gross nitrification pathways shifted across the pH gradient: heterotrophic nitrification was highest in acidic soils, while autotrophic nitrification became prevalent in calcareous soils, corresponding to increased ammonia-oxidizer abundances. The decreased importance of heterotrophic nitrification at higher pH was likely attributed to a decline in fungal populations, which are known to be the key drivers of this process (Zhang et al., 2020; Martikainen, 2022). At high pH, increased gross NH_4^+ production through organic N mineralization could have provided more substrate and stimulated the growth of AOA and AOB communities, thereby enhancing autotrophic nitrification (Yao et al., 2011; Song et al., 2016). Although, in the organic layer only AOA abundances showed a positive response to pH. Due to their high substrate affinity (Prosser and Nicol, 2012; Rütting et al., 2021), AOA may be more competitive. They may have primarily driven autotrophic nitrification in the organic layer, where intensive immobilization by heterotrophs has consumed most available NH_4^+.

In calcareous soils, increased gross nitrification, primarily contributed by the autotrophic process, leads to higher net NO_3^- release in the mineral topsoil. In the organic layer, when present, microbes immobilized all produced NO_3^-. Enhanced NO_3^- availability at high pH may benefit a wide range of calciphilic species that prefer NO_3^- (Falkengren-Grerup, 1995; Diekmann and Falkengren-Grerup, 1998). Species richness in Luxembourg forests strongly correlates with NO_3^- availability rather than NH_4^+ and NO_3^- combined (Kooijman, 2010). This pattern is consistent across temperate deciduous forests (Falkengren-Grerup and Schöttelndreier, 2004; Andrianarisoa et al., 2009). Therefore, in the studied beech forests, vegetation may profit from enhanced gross nitrification, which could lead to increased species richness at high pH.

6.3. Layer contributions to gross N transformations

The organic layer, when present, exhibited significantly higher rates of respiration (both on a C and areal basis), and more rapid turnover of both mineral and microbial N compared to the mineral topsoil. These findings align with previous temperate forest studies (Corre et al., 2003; Vervaet et al., 2004), suggesting high microbial activity and the importance of the organic layer in forest C and N flows. The contribution of the organic layer to gross N transformations is, however, gradually decreased along the pH gradient from acidic to calcareous soils, which reflects changes in decomposition and humus formation. In acidic soils, mor and mull-moder humus profiles with thick organic layers have developed from restricted soil animal activity and slow fungal decomposition (Kooijman et al., 2018a). In contrast, calcareous soils exhibit mull-type humus profiles with thin organic layers, and organic matter accumulates in mineral horizons due to earthworm activity and calcium-binding (Kooijman et al., 2009; Cammeraat et al., 2018). We observed increased soil organic matter, C, and N concentrations, and decreased C:N ratios in the mineral topsoil with rising pH. This pattern indicates increased decomposition and incorporation of organic matter (Hicks et al., 2021; Michalet and Liancourt, 2024), thereby enhancing the mineral topsoil's role in soil N transformations.

The mineral topsoil was the only layer contributing to net N release across the natural pH gradient. In acidic soils, limited immobilization led to low net release of both NH_4^+ and NO_3^- from gross mineralization and heterotrophic nitrification. In calcareous soils, high gross mineralization and nitrification contributed to high NO_3^- availability for plant roots, despite high microbial NH_4^+ immobilization.

6.4. Methodology limitations

In our laboratory incubation, soils were processed through sieving, mixing, and adjusting moisture levels to achieve homogeneous distribution of the ^{15}N tracer. This processing was necessary to mitigate the effects of soil spatial heterogeneity, which could otherwise introduce significant errors in calculating gross N fluxes (Wessel and Tietema, 1992; Murphy et al., 2003). However, it is likely that these steps disrupted soil microsites and increased C availability, potentially stimulating microbial activity and leading to an overestimation of gross N transformation rates (Booth et al., 2006; Staelens et al., 2012; He et al., 2020). This could explain the high gross mineralization rates compared to respiration rates. Microbial immobilization, particularly in the C-rich organic layer, may also have been enhanced, as longer-term net measurements using unsieved soils from the same sites showed net mineralization in both layers (Kooijman et al. 2008; Kooijman et al., 2016). Furthermore, the high tracer amount (50 mg N kg^{-1} soil) used to ensure accurate ^{15}N measurements may have artificially stimulated microbial immobilization, especially in calcareous mineral topsoil where initial NH_4^+ levels were low (<10 mg N kg^{-1} soil). This phenomenon is widely observed in studies employing the ^{15}N labelling method (Davidson et al., 1991; Corre et al., 2003; Ribbons et al., 2018). Thus, our results represent the "potential" gross N transformation rates rather than *in situ* activities (Watson et al., 2000; Accoe et al., 2004). Nevertheless, the rates we observed were within previously reported ranges from similar studies.

Soil processing may have also biased the relative contributions of fungi and bacteria to gross N transformations. Specifically, fungal-mediated immobilization might have been underestimated due to the disruption of fungal mycelia during sieving (Kubicek and Druzhinina, 2007; Li et al., 2019), particularly in the fungal-dominated acidic soils (He et al., 2020). This may have partially amplified the differences in gross immobilization between acidic and calcareous soils. Nevertheless, the observed increase in gross immobilization with bacterial dominance from acidic to calcareous soils likely reflects the general trend across the natural pH gradient. Our findings corroborate previous observations of declining net N mineralization in studies using both sieved (Andrianarisoa et al., 2009) and unsieved (Kooijman et al., 2008; Leberecht et al., 2016) soil samples, suggesting that high N demand by bacteria is a potential driver. Supporting this observation, de Vries et al. (2021) reported higher ^{15}N retention in intact soil cores from glacier foreland ecosystems with lower microbial C:N ratios.

In addition to AOA and AOB, comammox bacteria have been shown to be involved in autotrophic nitrification in various habitats, particularly in freshwater sediments and artificial ecosystems (e.g., sewage and agricultural soils) (Hu and He, 2017; Zhu et al., 2022). In temperate forests, comammox bacteria have also been found to be widely distributed (Wang et al., 2016), but their relative importance compared to ammonia nitrifiers remains unclear. A few studies suggested that comammox may be competitive in N-limited soils following forest disturbance (Osburn and Barrett, 2020) and can actively incorporate $^{13}CO_2$ in urea-fertilized eucalypt soils (Li et al., 2020). Since the forests in our study are neither N-limited nor fertilized, the role of comammox remains uncertain. If comammox bacteria have also been involved in autotrophic nitrification, the estimated contributions of AOA and AOB to NO_3^- availability across the pH gradient may be overestimated. Therefore, further investigations using qPCR and ^{13}C-DNA-SIP are thus needed to clarify the role of comammox in these forests.

7. Conclusions

Our study reveals distinct gross N transformation pathways in temperate beech forests across a natural pH gradient, closely tied to shifts in microbial community structure. As pH increases, gross mineralization, immobilization, and N turnover rates accelerated, reflecting the higher N demand of microbial communities dominated by bacteria. Concurrently, autotrophic nitrification increased with higher ammonia-oxidizer abundances at higher pH. In the mineral topsoil of calcareous soils, this resulted in increased NO_3^- availability for plant roots. In contrast, heterotrophic nitrification contributed most to gross nitrification in fungi-dominated acidic soils. These findings suggest that acidic and calcareous soils exhibit different strategies for supplying mineral N to vegetation through microbial transformations: low microbial immobilization in acidic soils and high gross nitrification in calcareous soils. Further studies using field ^{15}N tracing and involving other functional microbial groups, such as comammox, could further elucidate the contributions of the microbial community to internal N cycling and soil N supply under natural conditions.

CRediT authorship contribution statement

Mengru Jia: Writing – review & editing, Writing – original draft, Visualization, Validation, Resources, Methodology, Investigation, Formal analysis, Data curation, Conceptualization. **Annemieke Kooijman:** Writing – review & editing, Supervision, Resources, Conceptualization. **Roland Bol:** Conceptualization, Resources, Writing – review & editing, Supervision. **Wim W. Wessel:** Methodology, Resources, Software, Writing – review & editing. **Kathrin Hassler:** Writing – review & editing, Methodology, Formal analysis, Conceptualization. **Albert Tietema:** Writing – review & editing, Supervision, Resources, Conceptualization.

Declaration of competing interest

The authors declare that they have no known competing financial interests or personal relationships that could have appeared to influence the work reported in this paper.

Acknowledgement

We thank the staff of the physical and chemical laboratory and the molecular genetic laboratory of IBED for their invaluable expertise and assistance in the laboratory. Special thanks to Roselie Metz and Nicole van der Winden for their help in the field and with physical-chemical analysis. We also appreciate the support and suggestions of Dr. Relena Ribbons, Dr. Jingwei Fu, Lin Dong and Evy de Nijs during the molecular experiments. Additionally, we are grateful to Evy de Nijs for her assistance with editing the English text. Finally, we thank all the reviewers for their insightful and constructive feedback. Mengru Jia is supported by scholarship of China Scholarship Council (CSC, China) under the Grant CSC No. 201906190211.

Appendix A. Supplementary data

Supplementary data to this article can be found online at https://doi.org/10.1016/j.geoderma.2025.117194.

Data availability

Data will be made available on request.

References

Accoe, F., Boeckx, P., Busschaert, J., Hofman, G., Van Cleemput, O., 2004. Gross N transformation rates and net N mineralisation rates related to the C and N contents of soil organic matter fractions in grassland soils of different age. Soil Biol. Biochem. 36, 2075–2087. https://doi.org/10.1016/j.soilbio.2004.06.006.

Andrianarisoa, K.S., Zeller, B., Dupouey, J.L., Dambrine, E., 2009. Comparing indicators of N status of 50 beech stands (*Fagus sylvatica* L.) in northeastern France. For. Ecol. Manage. 257, 2241–2253. https://doi.org/10.1016/j.foreco.2009.02.037.

Andrianarisoa, K.S., Zeller, B., Poly, F., Siegenfuhr, H., Bienaimé, S., Ranger, J., Dambrine, E., 2010. Control of nitrification by tree species in a common-garden experiment. Ecosystems 13, 1171–1187. https://doi.org/10.1007/s10021-010-9390-x.

Baldrian, P., Větrovský, T., Cajthaml, T., Dobiášová, P., Petránková, M., Šnajdr, J., Eichlerová, I., 2013. Estimation of fungal biomass in forest litter and soil. Fungal Ecol. 6, 1–11. https://doi.org/10.1016/j.funeco.2012.10.002.

Barraclough, D., 1997. The direct or MIT route for nitrogen immobilization: A ^{15}N mirror image study with leucine and glycine. Soil Biol. Biochem. 29, 101–108. https://doi.org/10.1016/S0038-0717(96)00241-6.

Barraclough, D., 1991. The use of mean pool abundances to interpret ^{15}N tracer experiments. Plant and Soil 131, 89–96. https://doi.org/10.1007/BF00010423.

Bengtsson, G., Bengtson, P., Månsson, K.F., 2003. Gross nitrogen mineralization-, immobilization-, and nitrification rates as a function of soil C/N ratio and microbial activity. Soil Biol. Biochem. 35, 143–154. https://doi.org/10.1016/S0038-0717(02)00248-1.

Bergmann, G.T., Bates, S.T., Eilers, K.G., Lauber, C.L., Caporaso, J.G., Walters, W.A., Knight, R., Fierer, N., 2011. The under-recognized dominance of Verrucomicrobia in soil bacterial communities. Soil Biol. Biochem. 43, 1450–1455. https://doi.org/10.1016/j.soilbio.2011.03.012.

Berntson, G.M., Aber, J.D., 2000. Fast nitrate immobilization in N saturated temperate forest soils. Soil Biol. Biochem. 32, 151–156. https://doi.org/10.1016/S0038-0717(99)00132-7.

Booth, M.S., Stark, J.M., Hart, S.C., 2006. Soil-mixing effects on inorganic nitrogen production and consumption in forest and shrubland soils. Plant and Soil 289, 5–15. https://doi.org/10.1007/s11104-006-9083-6.

Booth, M.S., Stark, J.M., Rastetter, E., 2005. Controls on Nitrogen Cycling in Terrestrial Ecosystems: A Synthetic Analysis of Literature Data. Ecol. Monogr. 75, 139–157. https://doi.org/10.1890/04-0988.

Braun, J., Mooshammer, M., Wanek, W., Prommer, J., Walker, T.W.N., Rütting, T., Richter, A., 2018. Full ^{15}N tracer accounting to revisit major assumptions of ^{15}N isotope pool dilution approaches for gross nitrogen mineralization. Soil Biol. Biochem. 117, 16–26. https://doi.org/10.1016/j.soilbio.2017.11.005.

Brookes, P.C., Landman, A., Pruden, G., Jenkinson, D.S., 1985. Chloroform fumigation and the release of soil nitrogen: A rapid direct extraction method to measure microbial biomass nitrogen in soil. Soil Biol. Biochem. 17, 837–842. https://doi.org/10.1016/0038-0717(85)90144-0.

Cammeraat, L.H., Sevink, J., Hissler, C., Juilleret, J., Jansen, B., Kooijman, A.M., Pfister, L., Verstraten, J.M., 2018. Soils of the Luxembourg Lias Cuesta Landscape. In: Kooijman, A.M., Cammeraat, L.H., Seijmonsbergen, A.C. (Eds.), The Luxembourg Gutland Landscape, pp. 107–130, 10.1007/978-3-319-65543-7_6.

Caporaso, J.G., Lauber, C.L., Walters, W.A., Berg-Lyons, D., Lozupone, C.A., Turnbaugh, P.J., Fierer, N., Knight, R., 2011. Global patterns of 16S rRNA diversity at a depth of millions of sequences per sample. Proc. Natl. Acad. Sci. 108, 4516–4522. https://doi.org/10.1073/pnas.1000080107.

Cheng, Y., Wang, J., Mary, B., Zhang, J., Cai, Z., Chang, S.X., 2013. Soil pH has contrasting effects on gross and net nitrogen mineralizations in adjacent forest and grassland soils in central Alberta, Canada. Soil Biol. Biochem. 57, 848–857. https://doi.org/10.1016/j.soilbio.2012.08.021.

Clark, C.M., Richkus, J., Jones, P.W., Phelan, J., Burns, D.A., de Vries, W., Du, E., Fenn, M.E., Jones, L., Watmough, S.A., 2019. A synthesis of ecosystem management strategies for forests in the face of chronic nitrogen deposition. Environ. Pollut. 248, 1046–1058. https://doi.org/10.1016/j.envpol.2019.02.006.

Corre, M.D., Beese, F.O., Brumme, R., 2003. Soil Nitrogen Cycle in High Nitrogen Deposition Forest: Changes Under Nitrogen Saturation and Liming. Ecol. Appl. 13, 287–298. https://doi.org/10.1890/1051-0761(2003)013[0287:SNCIHN]2.0.CO;2.

Corre, M.D., Brumme, R., Veldkamp, E., Beese, F.O., 2007. Changes in nitrogen cycling and retention processes in soils under spruce forests along a nitrogen enrichment gradient in Germany. Glob. Chang. Biol. 13, 1509–1527. https://doi.org/10.1111/j.1365-2486.2007.01371.x.

Cox, G.M., Gibbons, J.M., Wood, A.T.A., Craigon, J., Ramsden, S.J., Crout, N.M.J., 2006. Towards the systematic simplification of mechanistic models. Ecol. Model. 198, 240–246. https://doi.org/10.1016/j.ecolmodel.2006.04.016.

Craine, J.M., Morrow, C., Fierer, N., 2007. Microbial Nitrogen Limitation Increases Decomposition. Ecology 88, 2105–2113. https://doi.org/10.1890/06-1847.1.

Dannenmann, M., Bimüller, C., Gschwendtner, S., Leberecht, M., Tejedor, J., Bilela, S., Gasche, R., Hanewinkel, M., Baltensweiler, A., Kögel-Knabner, I., Polle, A., Schloter, M., Simon, J., Rennenberg, H., 2016. Climate Change Impairs Nitrogen Cycling in European Beech Forests. PLoS One 11, e0158823. https://doi.org/10.1371/journal.pone.0158823.

Davidson, E.A., Hart, S.C., Firestone, M.K., 1992. Internal Cycling of Nitrate in Soils of a Mature Coniferous Forest. Ecology 73, 1148–1156. https://doi.org/10.2307/1940665.

Davidson, E.A., Hart, S.C., Shanks, C.A., Firestone, M.K., 1991. Measuring gross nitrogen mineralization, and nitrification by ^{15}N isotopic pool dilution in intact soil cores. J. Soil Sci. 42, 335–349. https://doi.org/10.1111/j.1365-2389.1991.tb00413.x.

de Graaff, M.-A., Classen, A.T., Castro, H.F., Schadt, C.W., 2010. Labile soil carbon inputs mediate the soil microbial community composition and plant residue decomposition rates. New Phytol. 188, 1055–1064. https://doi.org/10.1111/j.1469-8137.2010.03427.x.

de Vries, F.T., Bardgett, R.D., 2016. Plant community controls on short-term ecosystem nitrogen retention. New Phytol. 210, 861–874. https://doi.org/10.1111/nph.13832.
de Vries, F.T., Thion, C., Bahn, M., Bergk Pinto, B., Cécillon, S., Frey, B., Grant, H., Nicol, G.W., Wanek, W., Prosser, J.I., Bardgett, R.D., 2021. Glacier forelands reveal fundamental plant and microbial controls on short-term ecosystem nitrogen retention. J. Ecol. 109, 3710–3723. https://doi.org/10.1111/1365-2745.13748.
de Vries, F.T., van Groenigen, J.W., Hoffland, E., Bloem, J., 2011. Nitrogen losses from two grassland soils with different fungal biomass. Soil Biol. Biochem. 43, 997–1005. https://doi.org/10.1016/j.soilbio.2011.01.016.
Diao, M., Balkema, C., Suárez-Muñoz, M., Huisman, J., Muyzer, G., 2023. Succession of bacteria and archaea involved in the nitrogen cycle of a seasonally stratified lake. FEMS Microbiol. Lett. 370, fnad013. https://doi.org/10.1093/femsle/fnad013.
Diekmann, M., Falkengren-Grerup, U., 1998. A new species index for forest vascular plants: development of functional indices based on mineralization rates of various forms of soil nitrogen. J. Ecol. 86, 269–283. https://doi.org/10.1046/j.1365-2745.1998.00250.x.
Djemiel, C., Dequiedt, S., Bailly, A., Tripied, J., Lelièvre, M., Horrigue, W., Jolivet, C., Bispo, A., Saby, N., Valé, M., Maron, P.-A., Ranjard, L., Terrat, S., 2023. Biogeographical patterns of the soil fungal:bacterial ratio across France. mSphere 8, e00365–e00423. https://doi.org/10.1128/msphere.00365-23.
Elrys, A.S., Ali, A., Zhang, H., Cheng, Y., Zhang, J., Cai, Z.-C., Müller, C., Chang, S.X., 2021a. Patterns and drivers of global gross nitrogen mineralization in soils. Glob. Chang. Biol. 27, 5950–5962. https://doi.org/10.1111/gcb.15851.
Elrys, A.S., Uwiragiye, Y., Zhang, Y., Abdel-Fattah, M.K., Chen, Z., Zhang, H., Meng, L., Wang, J., Zhu, T., Cheng, Y., Zhang, J., Cai, Z., Chang, S.X., Müller, C., 2023. Expanding agroforestry can increase nitrate retention and mitigate the global impact of a leaky nitrogen cycle in croplands. Nat. Food 4, 109–121. https://doi.org/10.1038/s43016-022-00657-x.
Elrys, A.S., Wang, J., Metwally, M.A.S., Cheng, Y., Zhang, J.-B., Cai, Z.-C., Chang, S.X., Müller, C., 2021b. Global gross nitrification rates are dominantly driven by soil carbon-to-nitrogen stoichiometry and total nitrogen. Glob. Chang. Biol. 27, 6512–6524. https://doi.org/10.1111/gcb.15883.
Falkengren-Grerup, U., 1995. Interspecies differences in the preference of ammonium and nitrate in vascular plants. Oecologia 102, 305–311. https://doi.org/10.1007/BF00329797.
Falkengren-Grerup, U., Schöttelndreier, M., 2004. Vascular plants as indicators of nitrogen enrichment in soils. Plant Ecol. 172, 51–62. https://doi.org/10.1023/B:VEGE.0000026033.43070.e9.
Fisk, M.C., Schmidt, S.K., Seastedt, T.R., 1998. Topographic Patterns of Above- and Belowground Production and Nitrogen Cycling in Alpine Tundra. Ecology 79, 2253–2266. https://doi.org/10.1890/0012-9658(1998)079[2253:TPOAAB]2.0.CO;2.
Forest Europe, 2020.
Francis, C.A., Roberts, K.J., Beman, J.M., Santoro, A.E., Oakley, B.B., 2005. Ubiquity and diversity of ammonia-oxidizing archaea in water columns and sediments of the ocean. Proc. Natl. Acad. Sci. 102, 14683–14688. https://doi.org/10.1073/pnas.0506625102.
Gao, W., Chen, M., Xu, X., 2022. Tracing controls of autotrophic and heterotrophic nitrification in terrestrial soils. Eur. J. Soil Biol. 110, 103409. https://doi.org/10.1016/j.ejsobi.2022.103409.
Griffin, D.M., 1985. A comparison of the roles of bacteria and fungi. In: Leadbetter, E.R., Poindexter, J.S. (Eds.), Bacteria in Nature: Volume 1: Bacterial Activities in Perspective. Springer, US, Boston, MA, pp. 221–255. https://doi.org/10.1007/978-1-4615-6511-6_8.
Hart, S.C., Nason, G.E., Myrold, D.D., Perry, D.A., 1994a. Dynamics of gross nitrogen transformations in an old-growth forest: the carbon connection. Ecology 75, 880–891. https://doi.org/10.2307/1939413.
Hart, S.C., Stark, J.M., Davidson, E.A., Firestone, M.K., 1994b. Nitrogen mineralization, immobilization, and nitrification. In: Methods of Soil Analysis. John Wiley & Sons, Ltd, pp. 985–1018 doi: 10.2136/sssabookser5.2.c42.
He, X., Chi, Q., Cai, Z., Cheng, Y., Zhang, J., Müller, C., 2020. ^{15}N tracing studies including plant N uptake processes provide new insights on gross N transformations in soil-plant systems. Soil Biol. Biochem. 141, 107666. https://doi.org/10.1016/j.soilbio.2019.107666.
Hicks, L.C., Lajtha, K., Rousk, J., 2021. Nutrient limitation may induce microbial mining for resources from persistent soil organic matter. Ecology 102, e03328. https://doi.org/10.1002/ecy.3328.
Högberg, M.N., Blaško, R., Bach, L.H., Hasselquist, N.J., Egnell, G., Näsholm, T., Högberg, P., 2014. The return of an experimentally N-saturated boreal forest to an N-limited state: observations on the soil microbial community structure, biotic N retention capacity and gross N mineralisation. Plant and Soil 381, 45–60. https://doi.org/10.1007/s11104-014-2091-z.
Högberg, M.N., Chen, Y., Högberg, P., 2007. Gross nitrogen mineralisation and fungi-to-bacteria ratios are negatively correlated in boreal forests. Biol. Fertil. Soils 44, 363–366. https://doi.org/10.1007/s00374-007-0215-9.
Högberg, M.N., Myrold, D.D., Giesler, R., Högberg, P., 2006. Contrasting patterns of soil N-cycling in model ecosystems of Fennoscandian boreal forests. Oecologia 147, 96–107. https://doi.org/10.1007/s00442-005-0253-7.
Hu, H.-W., He, J.-Z., 2017. Comammox—a newly discovered nitrification process in the terrestrial nitrogen cycle. J. Soil. Sediment. 17, 2709–2717. https://doi.org/10.1007/s11368-017-1851-9.
Hu, X., Liu, C., Zheng, X., Dannenmann, M., Butterbach-Bahl, K., Yao, Z., Zhang, W., Wang, R., Cao, G., 2019. Annual dynamics of soil gross nitrogen turnover and nitrous oxide emissions in an alpine shrub meadow. Soil Biol. Biochem. 138, 107576. https://doi.org/10.1016/j.soilbio.2019.107576.
Jia, M., Bol, R., Kooijman, A., Wessel, W.W., Tietema, A., 2022. A decision support tool for the selection of ^{15}N analysis methods of ammonium and nitrate. Nutr. Cycl. Agroecosyst. https://doi.org/10.1007/s10705-022-10227-z.
Kausch, B., Maquil, R., 2018. Geological and geomorphological evolution of luxembourg and its cuesta landscape. In: Kooijman, A.M., Cammeraat, L.H., Seijmonsbergen, A.C. (Eds.), The Luxembourg Gutland Landscape. Springer International Publishing, pp. 1–19. https://doi.org/10.1007/978-3-319-65543-7_1.
Kooijman, A.M., 2010. Litter quality effects of beech and hornbeam on undergrowth species diversity in Luxembourg forests on limestone and decalcified marl. J. Veg. Sci. 21, 248–261. https://doi.org/10.1111/j.1654-1103.2009.01138.x.
Kooijman, A.M., Bloem, J., van Dalen, B.R., Kalbitz, K., 2016. Differences in activity and N demand between bacteria and fungi in a microcosm incubation experiment with selective inhibition. Appl. Soil Ecol. 99, 29–39. https://doi.org/10.1016/j.apsoil.2015.11.011.
Kooijman, A.M., Cammeraat, L.H., Seijmonsbergen, A.C. (Eds.), 2018a. The Luxembourg Gutland Landscape. Springer International Publishing, Cham, 10.1007/978-3-319-65543-7.
Kooijman, A.M., Kalbitz, K., Smit, A., 2018b. Alternative strategies for nutrient cycling in acidic and calcareous forests in the luxembourg cuesta landscape. In: Kooijman, A. M., Cammeraat, L.H., Seijmonsbergen, A.C. (Eds.), The Luxembourg Gutland Landscape. Springer International Publishing, Cham, pp. 131–151. https://doi.org/10.1007/978-3-319-65543-7_7.
Kooijman, A.M., Kooijman-Schouten, M.M., Martinez-Hernandez, G.B., 2008. Alternative strategies to sustain N-fertility in acid and calcaric beech forests: Low microbial N-demand versus high biological activity. Basic Appl. Ecol. 9, 410–421. https://doi.org/10.1016/j.baae.2007.05.004.
Kooijman, A.M., van Mourik, J.M., Schilder, M.L.M., 2009. The relationship between N mineralization or microbial biomass N with micromorphological properties in beech forest soils with different texture and pH. Biol. Fertil. Soils 45, 449–459. https://doi.org/10.1007/s00374-009-0354-2.
Krüger, M., Potthast, K., Michalzik, B., Tischer, A., Küsel, K., Deckner, F.F.K., Herrmann, M., 2021. Drought and rewetting events enhance nitrate leaching and seepage-mediated translocation of microbes from beech forest soils. Soil Biol. Biochem. 154, 108153. https://doi.org/10.1016/j.soilbio.2021.108153.
Kubicek, C.P., Druzhinina, I.S. (Eds.), 2007. Environmental and Microbial Relationships, The Mycota. Springer Berlin Heidelberg, Berlin, Heidelberg, pp. 47–68 doi:10.1007/978-3-540-71840-6_4.
Lachouani, P., Frank, A.H., Wanek, W., 2010. A suite of sensitive chemical methods to determine the $\delta^{15}N$ of ammonium, nitrate and total dissolved N in soil extracts: Preparation of soil N pools for natural ^{15}N abundance measurement. Rapid Commun. Mass Spectrom. 24, 3615–3623. https://doi.org/10.1002/rcm.4798.
Lang, F., Krüger, J., Kaiser, K., Bol, R., Loeppmann, S., 2021. Editorial: changes in forest ecosystem nutrition. Front. For. Global Change 4, 752063. https://doi.org/10.3389/ffgc.2021.752063.
Leberecht, M., Tu, J., Polle, A., 2016. Acid and calcareous soils affect nitrogen nutrition and organic nitrogen uptake by beech seedlings (*Fagus sylvatica* L.) under drought, and their ectomycorrhizal community structure. Plant Soil 409, 143–157. https://doi.org/10.1007/s11104-016-2956-4.
Li, C., Hu, H.-W., Chen, Q.-L., Chen, D., He, J.-Z., 2020. Niche differentiation of clade A comammox *Nitrospira* and canonical ammonia oxidizers in selected forest soils. Soil Biol. Biochem. 149, 107925. https://doi.org/10.1016/j.soilbio.2020.107925.
Li, J., Xie, T., Zhu, H., Zhou, J., Li, C., Xiong, W., Xu, L., Wu, Y., He, Z., Li, X., 2021. Alkaline phosphatase activity mediates soil organic phosphorus mineralization in a subalpine forest ecosystem. Geoderma 404, 115376. https://doi.org/10.1016/j.geoderma.2021.115376.
Li, X., He, H., Zhang, X., Yan, X., Six, J., Cai, Z., Barthel, M., Zhang, J., Necpalova, M., Ma, Q., Li, Z., 2019. Distinct responses of soil fungal and bacterial nitrate immobilization to land conversion from forest to agriculture. Soil Biol. Biochem. 134, 81–89. https://doi.org/10.1016/j.soilbio.2019.03.023.
Li, Y., Chapman, S.J., Nicol, G.W., Yao, H., 2018. Nitrification and nitrifiers in acidic soils. Soil Biol. Biochem. 116, 290–301. https://doi.org/10.1016/j.soilbio.2017.10.023.
Liu, Z., Lozupone, C., Hamady, M., Bushman, F.D., Knight, R., 2007. Short pyrosequencing reads suffice for accurate microbial community analysis. Nucleic Acids Res. 35, e120.
Luxhøi, J., Recous, S., Fillery, I.R.P., Murphy, D.V., Jensen, L.S., 2005. Comparison of $^{15}NH_4^+$ pool dilution techniques to measure gross N fluxes in a coarse textured soil. Soil Biol. Biochem. 37, 569–572. https://doi.org/10.1016/j.soilbio.2004.09.004.
Martikainen, P.J., 2022. Heterotrophic nitrification – An eternal mystery in the nitrogen cycle. Soil Biol. Biochem. 168, 108611. https://doi.org/10.1016/j.soilbio.2022.108611.
Mary, B., Recous, S., Robin, D., 1998. A model for calculating nitrogen fluxes in soil using 15N tracing. Soil Biol. Biochem. 30, 1963–1979. https://doi.org/10.1016/S0038-0717(98)00068-6.
Michalet, R., Liancourt, P., 2024. The interplay between climate and bedrock type determines litter decomposition in temperate forest ecosystems. Soil Biol. Biochem. 195, 109476. https://doi.org/10.1016/j.soilbio.2024.109476.
Murphy, D.V., Recous, S., Stockdale, E.A., Fillery, I.R.P., Jensen, L.S., Hatch, D.J., Goulding, K.W.T., 2003. Gross nitrogen fluxes in soil: theory, measurement and application of 15N pool dilution techniques. In: Advances in Agronomy. Elsevier, pp. 69–118 doi:10.1016/S0065-2113(02)79002-0.
Myrold, D.D., Tiedje, J.M., 1986. Simultaneous estimation of several nitrogen cycle rates using 15N: Theory and application. Soil Biol. Biochem. 18, 559–568. https://doi.org/10.1016/0038-0717(86)90076-3.
Neina, D., 2019. The role of soil pH in plant nutrition and soil remediation. Appl. Environ. Soil Sci. 2019, 5794869. https://doi.org/10.1155/2019/5794869.

Nordgren, A., 1988. Apparatus for the continuous, long-term monitoring of soil respiration rate in large numbers of samples. Soil Biol. Biochem. 20, 955–957. https://doi.org/10.1016/0038-0717(88)90110-1.
Osburn, E.D., Barrett, J.E., 2020. Abundance and functional importance of complete ammonia-oxidizing bacteria (comammox) versus canonical nitrifiers in temperate forest soils. Soil Biol. Biochem. 145, 107801. https://doi.org/10.1016/j.soilbio.2020.107801.
Payton, M.E., Miller, A.E., Raun, W.R., 2000. Testing statistical hypotheses using standard error bars and confidence intervals. Commun. Soil Sci. Plant Anal. https://doi.org/10.1080/00103620009370458.
Prosser, J.I., Nicol, G.W., 2012. Archaeal and bacterial ammonia-oxidisers in soil: the quest for niche specialisation and differentiation. Trends Microbiol. 20, 523–531. https://doi.org/10.1016/j.tim.2012.08.001.
Ribbons, R.R., Kepfer-Rojas, S., Kosawang, C., Hansen, O.K., Ambus, P., McDonald, M., Grayston, S.J., Prescott, C.E., Vesterdal, L., 2018. Context-dependent tree species effects on soil nitrogen transformations and related microbial functional genes. Biogeochemistry 140, 145–160. https://doi.org/10.1007/s10533-018-0480-8.
Ribbons, R.R., Levy-Booth, D.J., Masse, J., Grayston, S.J., McDonald, M.A., Vesterdal, L., Prescott, C.E., 2016. Linking microbial communities, functional genes and nitrogen-cycling processes in forest floors under four tree species. Soil Biol. Biochem. 103, 181–191. https://doi.org/10.1016/j.soilbio.2016.07.024.
Robertson, G.P., Groffman, P.M., 2024. Chapter 14 - Nitrogen transformations. In: Paul, E.A., Frey, S.D. (Eds.), Soil Microbiology, Ecology and Biochemistry, Fifth Edition. Elsevier, pp. 407–438. doi:10.1016/B978-0-12-822941-5.00014-4.
Roper, W.R., Robarge, W.P., Osmond, D.L., Heitman, J.L., 2019. Comparing four methods of measuring soil organic matter in North Carolina soils. Soil Sci. Soc. Am. J. 83, 466–474. https://doi.org/10.2136/sssaj2018.03.0105.
Rotthauwe, J.H., Witzel, K.P., Liesack, W., 1997. The ammonia monooxygenase structural gene amoA as a functional marker: molecular fine-scale analysis of natural ammonia-oxidizing populations. Appl. Environ. Microbiol. 63, 4704–4712. https://doi.org/10.1128/aem.63.12.4704-4712.1997.
Rousk, J., Frey, S.D., 2015. Revisiting the hypothesis that fungal-to-bacterial dominance characterizes turnover of soil organic matter and nutrients. Ecol. Monogr. 85, 457–472. https://doi.org/10.1890/14-1796.1.
Rütting, T., Cizungu Ntaboba, L., Roobroeck, D., Bauters, M., Huygens, D., Boeckx, P., 2015. Leaky nitrogen cycle in pristine African montane rainforest soil. Global Biogeochem. Cycles 29, 1754–1762. https://doi.org/10.1002/2015GB005144.
Rütting, T., Clough, T.J., Müller, C., Lieffering, M., Newton, P.C.D., 2010. Ten years of elevated atmospheric carbon dioxide alters soil nitrogen transformations in a sheep-grazed pasture. Glob. Chang. Biol. 16, 2530–2542. https://doi.org/10.1111/j.1365-2486.2009.02089.x.
Rütting, T., Huygens, D., Boeckx, P., Staelens, J., Klemedtsson, L., 2013. Increased fungal dominance in N2O emission hotspots along a natural pH gradient in organic forest soil. Biol. Fertil. Soils 49, 715–721. https://doi.org/10.1007/s00374-012-0762-6.
Rütting, T., Huygens, D., Staelens, J., Müller, C., Boeckx, P., 2011. Advances in ^{15}N-tracing experiments: new labelling and data analysis approaches. Biochem. Soc. Trans. 39, 279–283. https://doi.org/10.1042/BST0390279.
Rütting, T., Schleusner, P., Hink, L., Prosser, J.I., 2021. The contribution of ammonia-oxidizing archaea and bacteria to gross nitrification under different substrate availability. Soil Biol. Biochem. 160, 108353. https://doi.org/10.1016/j.soilbio.2021.108353.
Sanchez, G., Trinchera, L., Russolillo, G., 2017. plspm: tools for partial least squares path modeling (PLS-PM). R Package Version (4), 9.
Schimel, J., 1996. Assumptions and errors in the $^{15}NH_4^+$ pool dilution technique for measuring mineralization and immobilization. Soil Biol. Biochem. 28, 827–828.
Schmitz, A., Sanders, T.G.M., Bolte, A., Bussotti, F., Dirnböck, T., Johnson, J., Peñuelas, J., Pollastrini, M., Prescher, A.-K., Sardans, J., Verstraeten, A., de Vries, W., 2019. Responses of forest ecosystems in Europe to decreasing nitrogen deposition. Environ. Pollut. 244, 980–994. https://doi.org/10.1016/j.envpol.2018.09.101.
Scott, N.A., Parfitt, R.L., Ross, D.J., Salt, G.J., 1998. Carbon and nitrogen transformations in New Zealand plantation forest soils from sites with different N status. Can. J. For. Res. 28, 967–976. https://doi.org/10.1139/x98-067.
Sørensen, P., Jensen, E.S., 1991. Sequential diffusion of ammonium and nitrate from soil extracts to a polytetrafluoroethylene trap for ^{15}N determination. Anal. Chim. Acta 252, 201–203. https://doi.org/10.1016/0003-2670(91)87215-S.
Staelens, J., Rütting, T., Huygens, D., De Schrijver, A., Müller, C., Verheyen, K., Boeckx, P., 2012. In situ gross nitrogen transformations differ between temperate deciduous and coniferous forest soils. Biogeochemistry 108, 259–277. https://doi.org/10.1007/s10533-011-9598-7.
Stark, J.M., Hart, S.C., 1997. High rates of nitrification and nitrate turnover in undisturbed coniferous forests. Nature 385, 61–64. https://doi.org/10.1038/385061a0.
Strickland, M.S., Rousk, J., 2010. Considering fungal:bacterial dominance in soils – Methods, controls, and ecosystem implications. Soil Biol. Biochem. 42, 1385–1395. https://doi.org/10.1016/j.soilbio.2010.05.007.
Tahovská, K., Kaňa, J., Bárta, J., Oulehle, F., Richter, A., Šantrůčková, H., 2013. Microbial N immobilization is of great importance in acidified mountain spruce forest soils. Soil Biol. Biochem. 59, 58–71. https://doi.org/10.1016/j.soilbio.2012.12.015.
Templer, P.H., Mack, M.C., Chapin, F.S., Christenson, L.M., Compton, J.E., Crook, H.D., Currie, W.S., Curtis, C.J., Dail, D.B., D'Antonio, C.M., Emmett, B.A., Epstein, H.E., Goodale, C.L., Gundersen, P., Hobbie, S.E., Holland, K., Hooper, D.U., Hungate, B.A., Lamontagne, S., Nadelhoffer, K.J., Osenberg, C.W., Perakis, S.S., Schleppi, P., Schimel, J., Schmidt, I.K., Sommerkorn, M., Spoelstra, J., Tietema, A., Wessel, W.W., Zak, D.R., 2012. Sinks for nitrogen inputs in terrestrial ecosystems: a meta-analysis of ^{15}N tracer field studies. Ecology 93, 1816–1829. https://doi.org/10.1890/11-1146.1.
Tietema, A., 1992. Nitrogen cycling and soil acidification in forest ecosystems in the Netherlands.
Tietema, A., Wessel, W.W., 1992. Gross nitrogen transformations in the organic layer of acid forest ecosystems subjected to increased atmospheric nitrogen input. Soil Biol. Biochem. 24, 943–950. https://doi.org/10.1016/0038-0717(92)90021-O.
Vance, E.D., Brookes, P.C., Jenkinson, D.S., 1987. An extraction method for measuring soil microbial biomass C. Soil Biol. Biochem. 19, 703–707. https://doi.org/10.1016/0038-0717(87)90052-6.
Verchot, L.V., Holmes, Z., Mulon, L., Groffman, P.M., Lovett, G.M., 2001. Gross vs net rates of N mineralization and nitrification as indicators of functional differences between forest types. Soil Biol. Biochem. 33, 1889–1901. https://doi.org/10.1016/S0038-0717(01)00095-5.
Vervaet, H., Boeckx, P., Boko, A.M.C., Van Cleemput, O., Hofman, G., 2004. The role of gross and net N transformation processes and NH_4^+ and NO_3^- immobilization in controlling the mineral N pool of a temperate mixed deciduous forest soil. Plant and Soil 264, 349–357. https://doi.org/10.1023/B:PLSO.0000047766.16919.5e.
Vitousek, P.M., Treseder, K.K., Howarth, R.W., Menge, D.N.L., 2022. A "toy model" analysis of causes of nitrogen limitation in terrestrial ecosystems. Biogeochemistry 160, 381–394. https://doi.org/10.1007/s10533-022-00959-z.
de Vries, F.T., Bloem, J., Quirk, H., Stevens, C.J., Bol, R., Bardgett, R.D., 2012. Extensive management promotes plant and microbial nitrogen retention in temperate grassland. PLoS One 7, e51201. https://doi.org/10.1371/journal.pone.0051201.
Wakelin, S.A., Colloff, M.J., Harvey, P.R., Marschner, P., Gregg, A.L., Rogers, S.L., 2007. The effects of stubble retention and nitrogen application on soil microbial community structure and functional gene abundance under irrigated maize. FEMS Microbiol. Ecol. 59, 661–670. https://doi.org/10.1111/j.1574-6941.2006.00235.x.
Wang, J.-T., Zheng, Y.-M., Hu, H.-W., Li, J., Zhang, L.-M., Chen, B.-D., Chen, W.-P., He, J.-Z., 2016. Coupling of soil prokaryotic diversity and plant diversity across latitudinal forest ecosystems. Sci. Rep. 6, 19561. https://doi.org/10.1038/srep19561.
Watson, C.J., Travers, G., Kilpatrick, D.J., Laidlaw, A.S., O'Riordan, E., 2000. Overestimation of gross N transformation rates in grassland soils due to non-uniform exploitation of applied and native pools. Soil Biol. Biochem. 32, 2019–2030. https://doi.org/10.1016/S0038-0717(00)00103-6.
Wessel, W.W., Tietema, A., 1992. Calculating gross N transformation rates of ^{15}N pool dilution experiments with acid forest litter: Analytical and numerical approaches. Soil Biol. Biochem. 24, 931–942. https://doi.org/10.1016/0038-0717(92)90020-X.
White, T.J., Bruns, T., Lee, S., Taylor, J., 1990. Amplification and direct sequencing of fungal ribosomal RNA genes for phylogenetics. In: PCR Protocols: A Guide to Methods and Applications, pp. 315–322.
Zhalnina, K., Dias, R., de Quadros, P.D., Davis-Richardson, A., Camargo, F.A.O., Clark, I.M., McGrath, S.P., Hirsch, P.R., Triplett, E.W., 2015. Soil pH determines microbial diversity and composition in the park grass experiment. Microb. Ecol. 69, 395–406. https://doi.org/10.1007/s00248-014-0530-2.
Zhang, B., Zhou, M., Zhu, B., Xiao, Q., Zheng, X., Zhang, J., Müller, C., Butterbach-Bahl, K., 2022. Soil clay minerals: An overlooked mediator of gross N transformations in Regosolic soils of subtropical montane landscapes. Soil Biol. Biochem. 168, 108612. https://doi.org/10.1016/j.soilbio.2022.108612.
Zhang, J., Cai, Z., Müller, C., 2018. Terrestrial N cycling associated with climate and plant-specific N preferences: a review: Soil N cycle in relation to climate and plant N preferences. Eur. J. Soil Sci. 69, 488–501. https://doi.org/10.1111/ejss.12533.
Zhang, Y., Cai, Z., Zhang, J., Müller, C., 2023. The controlling factors and the role of soil heterotrophic nitrification from a global review. Appl. Soil Ecol. 182, 104698. https://doi.org/10.1016/j.apsoil.2022.104698.
Zhang, Y., Dai, S., Huang, X., Zhao, Y., Zhao, J., Cheng, Y., Cai, Z., Zhang, J., 2020. pH-induced changes in fungal abundance and composition affects soil heterotrophic nitrification after 30 days of artificial pH manipulation. Geoderma 366, 114255. https://doi.org/10.1016/j.geoderma.2020.114255.
Zhu, G., Wang, X., Wang, S., Yu, L., Armanbek, G., Yu, J., Jiang, L., Yuan, D., Guo, Z., Zhang, H., Zheng, L., Schwark, L., Jetten, M.S.M., Yadav, A.K., Zhu, Y.-G., 2022. Towards a more labor-saving way in microbial ammonium oxidation: A review on complete ammonia oxidization (comammox). Sci. Total Environ. 829, 154590. https://doi.org/10.1016/j.scitotenv.2022.154590.